

Study of mining contamination by heavy metals and metalloids in soils

Marcus Vinícius Pereira da Silva Monteiro

Master's degree in chemistry

Department of chemistry and biochemistry

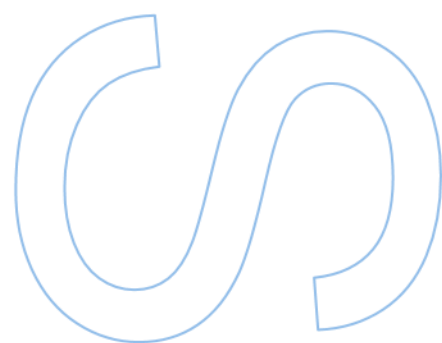
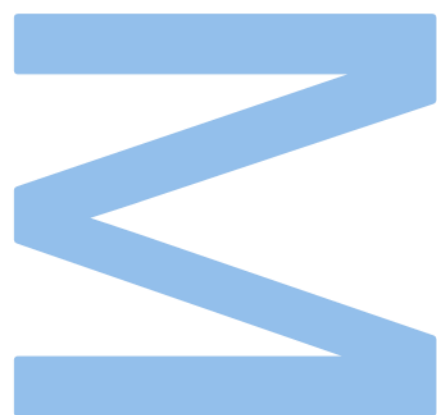
2022

Supervisor

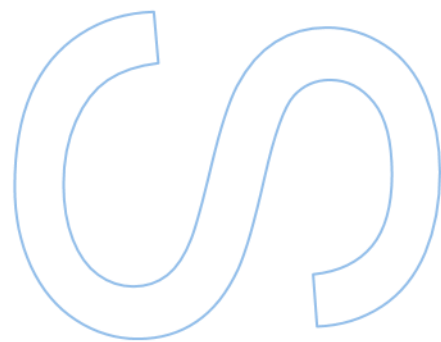
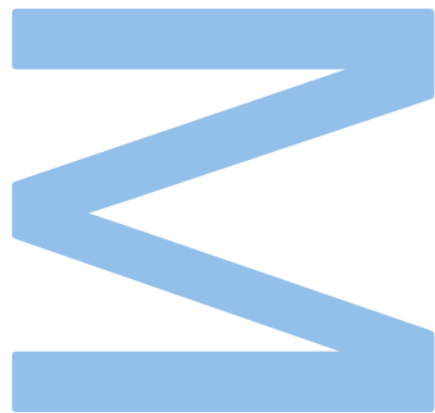
Manuel Augusto Gomes de Oliveira Azenha, Auxiliar professor, Faculty of Sciences of University of Porto

Co-supervisor

José Adolfo Oliveira Ribeiro, Reseacher, Faculty of Sciences of University of Porto



U. PORTO
FC FACULDADE DE CIÊNCIAS
UNIVERSIDADE DO PORTO



Sworn Statement

I, Marcus Vinícius Pereira da Silva Monteiro, enrolled in the Master Degree in Chemistry at the Faculty of Sciences of the University of Porto hereby declare, in accordance with the provisions of paragraph a) of Article 14 of the Code of Ethical Conduct of the University of Porto, that the content of this dissertation reflects perspectives, research work and my own interpretations at the time of its submission.

By submitting this dissertation, I also declare that it contains the results of my own research work and contributions that have not been previously submitted to this or any other institution.

I further declare that all references to other authors fully comply with the rules of attribution and are referenced in the text by citation and identified in the bibliographic references section. This dissertation does not include any content whose reproduction is protected by copyright laws.

I am aware that the practice of plagiarism and self-plagiarism constitute a form of academic offense.

Marcus Vinícius Pereira da Silva Monteiro

09/30/2022

Acknowledgements

I would like to take this opportunity to express my immense gratitude to all those people who have given their invaluable support and assistance.

My sincere thanks to my supervisor Prof. Dr. Manuel Azenha and my co-supervisor Dr. José Ribeiro for the possibility of working on this thesis, for the continuous support, teachings and for all the trust in my skills and capabilities.

To Prof. Dr. Carlos Pereira for also believing in my capacities and for all the meetings organized for the research group.

To all the members of the research group I was part of during this period for all the kindness and support.

To my friends of the university and the ones across the ocean that accompanied and supported me through this year providing moments fun and relaxation.

To my family for all the effort and support provided to finish this thesis.

To the project SHS (NORTE-01-0145-FEDER-000056) for the financial support.

Resumo

Este trabalho tem como objetivo estudar a presença e disseminação de espécies de mercúrio provenientes de resíduos produzidos por duas minas atualmente desativadas, o complexo mineiro de Pejão, localizado em Castelo de Paiva, e a mina Poça da Cadela de W-Sb, localizada em Regoufe, fornecendo informações sobre os riscos impostos pelo mercúrio para o ambiente e potencialmente para a saúde humana.

A abordagem consistiu em primeiramente submeter sub-amostras de solo a um processo de digestão com aplicação da tecnologia micro-ondas, utilizando *aqua regia*, para obter o conteúdo total de mercúrio no solo. Contudo, a biodisponibilidade e toxicidade de elementos potencialmente tóxicos (PTEs, do inglês *Potentially Toxic Elements*) para os organismos é fortemente influenciada pelas formas químicas em que estes se encontram no ambiente (especificação). Portanto, neste trabalho foi aplicado um procedimento de extração sequencial (SEP, do inglês *Sequential Extraction Procedure*), descrito na norma da EPA (do inglês *Environmental Protection Agency*, Estados Unidos) 3200, de modo permitir fracionar o Hg presente no solo em três frações: móvel, semi-móvel e não-móvel, sendo a fração móvel a mais preocupante do ponto de vista ambiental uma vez que contém as espécies de mercúrio mais lábeis e tóxicas.

Neste trabalho, a deteção de Hg nos extratos obtidos foi realizada utilizando a técnica de espectroscopia de absorção atômica com geração de vapor a frio (CV-AAS, do inglês *Cold Vapor Atomic Absorption Spectroscopy*). Para isso, foi utilizado um sistema gerador de vapor automatizado em fluxo contínuo, o acessório VP100, para gerar o vapor frio de Hg. Assim sendo, a primeira parte deste trabalho teve como foco a seleção dos reagentes (agente redutor e ácido), e suas respectivas concentrações, para a formação do vapor frio, assim como a otimização dos parâmetros instrumentais do VP100, nomeadamente a velocidade da bomba e o caudal de gás inerte (N₂). O procedimento experimental foi alterado de forma a minimizar o consumo de amostra sem, contudo, afetar a sensibilidade do método para quantificação do mercúrio.

Para a determinação do mercúrio nos extratos do solo, foram utilizadas soluções padrão de Hg de concentração 2,00, 5,00, 10,0, 15,0 e 20,0 $\mu\text{g.L}^{-1}$ para construir curvas de calibração. As curvas de calibração foram preparadas diariamente e alguns parâmetros analíticos determinados. O limite de deteção (LOD) obtido foi de 0,3 $\mu\text{g.L}^{-1}$, o limite de quantificação (LOQ) de 1,0 $\mu\text{g.L}^{-1}$ (usando um nível de confiança de 95%), e a sensibilidade do método foi de 0,5 $\mu\text{g.L}^{-1}$.

Os resultados obtidos demonstraram um enriquecimento em Hg no solo da região da escombreira do Fojo, variando de 0,1 a 1,2 mg.kg⁻¹, relativamente aos valores de referência regionais e nacionais devido à atividade antropogénica, com níveis de concentração superiores ao valor de referência reportados pela Agência Portuguesa do Ambiente (APA) para solos de uso agrícola (0,25 mg.kg⁻¹) na zona da escombreira e na região a jusante.

O método de extração sequencial (SEP) revelou uma predominância de espécies de mercúrio encontradas na fração semi-móvel (tais como complexos de Hg²⁺ e amálgamas de metais com Hg⁰) com uma concentração média de mercúrio de 0,5 mg.kg⁻¹, ou seja, uma predominância de espécies de mercúrio menos biodisponíveis para os solos e aquíferos circundantes. Contudo, é aconselhável o controlo e monitorização ambiental da região, uma vez que algumas amostras apresentaram níveis de Hg próximos do valor de referência APA na fração móvel, que contém as espécies mais tóxicas e biodisponíveis (como o HgSO₄ e CH₃Hg⁺). Através de um teste estatístico foi também possível concluir que a combustão da pilha de resíduos, em 2017, fez aumentar a biodisponibilidade do mercúrio nesta região provavelmente devido à decomposição térmica dos materiais e espécies de mercúrio principalmente encontradas na fração não-móvel.

Relativamente à mina de Regoufe, a região foi classificada como "moderada a extremamente contaminada" de acordo com os valores do índice de geoacumulação obtidos para o Hg. Os resultados revelaram também um enriquecimento deste PTE nas amostras de solo recolhidas quando comparadas com os valores de referências reportados para Portugal, com a concentração de mercúrio variando de 0,4 a 6,9 mg.kg⁻¹ entre amostras.

Para esta região, os resultados do procedimento de extração sequencial (SEP) revelaram uma elevada concentração das espécies mais lábeis de Hg (por exemplo, o HgSO₄) em algumas amostras de solo, nomeadamente as amostras R2, R4, R7 e R14. No entanto, foram encontrados valores de recuperação muito baixos (aproximadamente 30%) após a aplicação do SEP na região de Regoufe. Assim sendo, e antes das conclusões finais, são necessários ensaios adicionais para confirmar e compreender os resultados obtidos para esta região mineira.

Assim sendo, os dados obtidos para a avaliação do risco de Hg evidenciaram o impacto ambiental negativo da atividade mineira nas regiões estudadas, enfatizando o risco ambiental decorrente dos resíduos mineiros não tratados e expostos ao ambiente

e a necessidade de controlo e monitorização dos metais pesados e de intervenção para a remediação da contaminação nessas regiões.

Palavras-chave: mercúrio, metais pesados, solo de mina, contaminação do solo, extração sequencial, espectroscopia de absorção atómica com geração de vapor a frio.

Abstract

This work aims to study the presence and dissemination of mercury species from residues produced by two currently deactivated mines, the Pejão mining complex, located in Castelo de Paiva, and the Poça da Cadela W-Sb mine, located in Regoufe, providing information about the risks imposed by mercury to the environment and potentially to human health.

The approach consisted to first subjecting soil sub-samples to microwave-assisted digestion with *aqua regia* to obtain the total content of mercury in the soil. Moreover, potentially toxic elements (PTEs) bioavailability and toxicity to organisms is strongly influenced by the chemical forms in which PTEs are found in the environment. Thus, in this work, a sequential extraction procedure (SEP), the USEPA 3200, was applied to fractionate Hg in soils into three fractions: mobile, semi-mobile and non-mobile, here the mobile fraction is the most concerning one since it contains the most labile mercury species.

In this work, Hg detection in sample extracts was performed using cold vapor atomic absorption spectroscopy (CV-AAS) method. For that, an automated continuous flow system, the VP100 accessory, was used to generate the cold vapor. The first part of this work focused on the selection of the chemical reagents (reducing agent and acid) and their concentration and optimization of instrumental parameters, namely the pump speed and inert gas (N₂) flow rate, for the quantification of mercury. In addition, the procedure was adapted to minimize sample consumption without compromising detection sensitivity.

Standard solutions of 2.00, 5.00, 10.0, 15.0 and 20.0 µg.L⁻¹ were used to build the daily calibration curve for Hg analysis. For a typical calibration curve obtained some analytical parameters were estimated. The method detection limit (LOD) was 0.3 µg.L⁻¹ and the quantification limit (LOQ) was 1.0 µg.L⁻¹ (for 95% confidence), with a sensitivity of 0.5 µg.L⁻¹.

For the Fojo waste pile, the results obtained demonstrated an enrichment of Hg in this region relatively to regional and national background values due to anthropogenic activity, with concentration levels ranging from 0.1 to 1.2 mg.kg⁻¹ exceeding “*Agência Portuguesa do Ambiente*” (APA) reference value for agricultural use soils (0.25 mg.kg⁻¹) at the waste pile and at the downstream region.

The SEP applied to soil samples from this region revealed a predominance of mercury species found at the semi-mobile fraction (such as Hg^{2+} complexes and Hg^0 -metal amalgams) with an average mercury concentration of 0.5 mg.kg^{-1} , that is, a predominance of less readily bioavailable species for surrounding soils and aquifers. However, control and monitoring of the region may be advisable since some samples presented levels of Hg close to the APA reference value in the mobile-fraction, that contains the most toxic and bioavailable species (such as HgSO_4 and CH_3Hg^+). Furthermore, through a statistical test it was also possible to conclude that the combustion of the waste pile, in 2017, probably contributed to increase the mercury bioavailability in this region due to the thermal decomposition of mercury species mainly found in the non-mobile fraction.

Relatively to the Regoufe mine, the region was classified as “moderated to extremely contaminated” according to the geoaccumulation index values obtained for Hg. The results also revealed an enrichment of this PTE in the mine soil samples collected when compared to Portugal background values, with the mercury concentration ranging from 0.4 to 6.9 mg.kg^{-1} between samples.

The SEP results revealed a threatening contamination of the mine area due to the high concentration of Hg (above APA reference value) in the mobile-fraction for some soil samples, namely samples R2, R4, R7 and R14. Nonetheless, a critical limitation was encountered on the application of the SEP in the Regoufe region. Very low recovery values were obtained (approximately 30%), and thus further assays should be performed to confirm and fully understand the results obtained for this mine region.

Therefore, the obtained data for the risk assesment of Hg revealed the negative environmental impact of the mining activity in the studied regions emphasizing the environmental risk arising from untreated and exposed mine wastes and the need for control and monitoring of heavy metals and intervention for the remediation of the contamination in those regions.

Key words: mercury, heavy metals, mine soil, soil contamination, sequential extraction, cold vapor atomic absorption spectroscopy.

Table of Contents

List of Tables.....	x
List of Figures.....	xi
List of Abbreviations	xiii
1. Introduction.....	1
1.1. Framework	1
1.2. Soil contamination by heavy metals.....	2
1.3. Study areas	3
1.3.1. Fojo waste pile of the Pejão mining complex.....	3
1.3.2. Poça da Cadela mine in Regoufe.....	4
1.4. Mercury toxicity and bioavailability.....	5
1.5. Mercury sequential extraction procedure – USEPA 3200	5
1.6. Mercury extraction and determination.....	7
1.6.1. Soil sample preparation	8
1.6.2. Mercury Determination by CV-AAS.....	8
1.7. Atomic absorption spectrometry	9
1.7.1. Process of atomic absorption.....	9
1.7.2. Atomic absorption instrument.....	10
1.7.3. Hydride generation technique	12
1.7.4. Mercury cold vapor technique	12
1.8. Objectives	13
2. Materials and methods	14
2.1. Safety measures	14
2.2. Soil sampling and processing.....	14
2.3. Materials, instruments, reagents and solvents.....	16
2.3.1. Common labware.....	16
2.3.2. Common lab instruments	17
2.3.3. Reagents and solvents.....	17

2.4. Soil sample digestion with <i>aqua regia</i>	18
2.5. Mercury sequential extraction procedure	20
2.5.1. Extraction solutions	20
2.5.2. Extraction of mobile mercury – Step 1.....	20
2.5.3. Extraction of semi-mobile mercury – Step 2.....	21
2.5.4. Extraction of non-mobile mercury – Step 3.....	22
2.6. Mercury analysis by Cold Vapor Atomic Absorption Spectrometry (CV-AAS) ...	23
2.6.1 Instrumentation	23
2.6.2. Solutions for Cold Vapor/Hydride generation	24
2.6.3 Operation conditions	25
2.6.4 Calibration curve for mercury and analytical parameters.....	25
3. Results and discussion	30
3.1. Optimization of experimental conditions for cold vapor/hydride generation.....	30
3.1.2. Chemical variables optimization	30
3.1.1. VP100 instrument variables optimization	31
3.2. Hg measurement and calibration curve for Hg quantification	33
3.3. Case of study: Fojo waste pile of Pejão mining complex	36
3.3.1. <i>Aqua regia</i> extractable content of Hg in soil samples.....	36
3.3.2. Mercury fractionating	41
3.4. Case of study: Poça da cadela wolframium mine in Regoufe	44
3.4.1. <i>Aqua regia</i> extractable content of Hg in soil samples.....	44
3.4.2. Mercury fractioning	48
4. Conclusions and future work.....	52
5. Bibliography.....	55
Annex I – Preliminary results for As and Sb	61
Annex II – As and Sb SEP method.....	63

List of Tables

Table 1 - Operationally defined fractions and related extracted species.	6
Table 2 - Reagents and solvents used.	18
Table 3 - Operating condition for microwave digestion procedure.....	18
Table 4 - Decontamination procedure operating conditions.	20
Table 5 - Operating conditions of the CV-AAS system.....	25
Table 6 - Preliminary assays results for instrumental optimization.	32
Table 7 - Calculated analytical parameters.....	35
Table 8 - Hg <i>aqua regia</i> soluble content in Pejão coal mine samples (EA, ENA, B and SJ).	37
Table 9 - Geoaccumulation index classification chart.	40
Table 10 - Calculated geoaccumulation index for all Pejão coal mine samples (EA, ENA, B and SJ).	41
Table 11 - Hg concentration (mg.kg ⁻¹) in each extracted fraction for Pejão coal mine samples (EA, ENA, B and SJ).....	42
Table 12 - Hg <i>aqua regia</i> soluble content for Regoufe mine samples	45
Table 13 - Calculated geoaccumulation index for all Regoufe mine samples.....	48
Table 14 - Hg concentration (mg.kg ⁻¹) in each extracted fraction for Regoufe mine samples.	49
Table 15 - Hg <i>aqua regia</i> soluble content for Regoufe mine samples.	61

List of Figures

Figure 1 - Left: Fojo waste pile region during EDM intervention to stop the fire; Right: Waste pile after being affected by the fire.	4
Figure 2 – Different angles of the deactivated W-Sb Poça de Cadela mining complex and some of its residue piles in Regoufe.....	4
Figure 3 - State transitions by excitation or decay. (Adapted from reference 32).....	10
Figure 4 - Diagram of an atomic absorption spectrometer instrument (Figure from reference [32]).	11
Figure 5 - Hollow cathode lamp scheme (Figure from reference [32])	11
Figure 6 - Diagram of AAS instrument setup for CV-AAS analysis (Figure adapted from reference [32]).	13
Figure 7 - Sample distribution map in Fojo region.	15
Figure 8 - Sample distribution map in Regoufe region.....	16
Figure 9 - Microwave-assisted digestion system consisting of oven, rotor and vessels.	19
Figure 10 - Scheme of the ultrasound bath used in the first extraction step.....	21
Figure 11 - Representative scheme of the water bath system used in the second extraction step.	22
Figure 12 - VP100 (left) and atomic absorption <i>spectrometer</i> (right) used for CV-AAS measurements.	23
Figure 13 - Absorption cell used in this work for determination of mercury.	24
Figure 14 - Typical graphical representation of absorbance versus time obtained for a 20.0 $\mu\text{g.L}^{-1}$ Hg solution. The total measurement time was 100 s.	26
Figure 15 - Typical calibration curve obtained for the determination of mercury by using peak height as analytical signal. Standard solutions of 2.00, 5.00,10.0, 15.0 and 20.0 mg.kg^{-1} were used.	34
Figure 16 - Typical calibration curve obtained for the determination of mercury by using peak area as analytical signal. Standard solutions of 2.00, 5.00,10.0, 15.0 and 20.0 mg.kg^{-1} were used.	34
Figure 17 - Graphical representation of the obtained aqua regia soluble content of Hg in Pejão coal mine samples (EA, ENA, B and SJ). APA reference value represented by the red line.....	38
Figure 18 - Map of colors of Hg distribution in Fojo waste pile and surrounding region.	39

Figure 19 – Graphical representation of Hg concentration (mg.kg^{-1}) in each extracted fraction for Pejão coal mine samples (EA, ENA, B and SJ)..... 43

Figure 20 - Graphical representation of the obtained *aqua regia* soluble content of Hg in Pejão coal mine samples. APA reference value represented by the red line..... 46

Figure 21 - Map of colors of Hg distribution in Fojo waste pile and surrounding region. 47

Figure 22 - Graphical representation of Hg concentration (mg.kg^{-1}) in each extracted fraction for Regoufe mine samples..... 50

List of Abbreviations

AAS	ATOMIC ABSORPTION SPECTROSCOPY
AMD	ACID MINE DRAINAGE
APA	<i>AGÊNCIA PORTUGUESA DO AMBIENTE</i>
BCR	COMMUNITY BUREAU OF REFERENCE
CV-AAS	COLD VAPOR ATOMIC ABSORPTION SPECTROSCOPY
EDM	<i>EMPRESA DE DESENVOLVIMENTO MINEIRO</i>
ET-AAS	ELETRO THERMAL ATOMIC ABSORPTION SPECTROSCOPY
HG-AAS	HYDRIDE GENERATION ATOMIC ABSORPTION SPECTROSCOPY
ICP-MS	INDUCTIVELY COUPLED PLASMA MASS SPECTROSCOPY
LOD	LIMIT OF DETECTION
LOQ	LIMIT OF QUANTIFICATION
MAX	MAXIMUM
MIN	MINIMUM
PTE	POTENTIALLY TOXIC ELEMENT
SD	STANDARD DEVIATION
SEP	SEQUENTIAL EXTRACTION PROCEDURE
USEPA	UNITED STATES ENVIRONMENTAL PROTECTION AGENCY

1. Introduction

1.1. Framework

This work was carried out under the scope of the multidisciplinary research project “SHS - Soil health surrounding former mining areas: characterization, risk analysis, and intervention” that aims to identify environmental impacts related with the residues produced by currently deactivated mines, namely the Fojo waste piles of the Pejão coal mine complex and the Sb-W mine Poça da Cadela in Regoufe.

The contribution of CIQUP research center to the research project rely on assessing heavy metals (Hg, As, Sb, Ni, Cd, Cr, Pb, Zn and Cu) bioavailability and speciation in mine soils. The work is performed in close collaboration with the department of Geosciences, Environment and Spatial Plannings of University of Porto, that is responsible for collecting, pre-treating and supplying the soil samples from the mine regions. In this context, the collected mine soil samples were sent to an international laboratory to assess the total concentration of several heavy metals by ICP-MS (external service). However, mercury is not included in those results. Therefore, due to a lack of information about this very concerning PTE, this work focused mainly on Hg determination and fractioning in mine regions soils.

In the present work, the potential environmental impact of mercury in mine soils was investigated by first digesting sub-samples of the collected soil through a microwave-assisted procedure using *aqua regia* to assess the total mercury content. Then, a sequential extraction procedure (USEPA 3200) was applied to assess Hg speciation and bioavailability, aiming to provide a more reliable scenario about the potential risk of this contaminant to the mine surrounding ecosystems. For quantification of trace mercury concentration on the obtained extracts, cold vapor atomic absorption spectroscopy (CV-AAS) technique was used.

Nonetheless, some results of this work were already presented in national and international conferences:

- (i) **Oral presentation** - Speciation of metals and metalloids in soils of deactivated mining areas by sequential extraction procedures, M. Monteiro, J. Ribeiro, M. Azenha, Jornadas do ICT 2022, February 10-11, 2022
- (ii) **Oral presentation** - Speciation of Mercury in Soils of a Deactivated Mining Area by a Sequential Extraction Procedure, M. Monteiro, José A. Ribeiro, M. Azenha, 15th IJUP, Porto, Portugal, May 4-6, 2022.

- (iii) **Conference paper/Poster** - Potentially toxic elements in mining waste affected by coal fires in a Douro Coalfield waste pile, P. Santos, M. Monteiro, J.A. Ribeiro, C. Pereira, J. Espinha Marques, J. Ribeiro, M. Azenha, D. Flores, XIII National Congress and XIII Iberian Congress of Geochemistry, Puertollano, Spain, April 25-27, 2022.

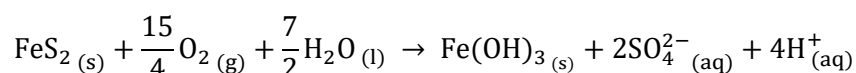
1.2. Soil contamination by heavy metals

Heavy metals, also referred in the literature as “potentially toxic elements (PTEs)”, are classified as metals whose density is higher than 5 g.cm^{-3} and that pose a risk to the environment and to living organisms.^[1] Although some heavy metals are essential for some plants and animals to maintain their biological processes (i.e. Zn and Cu), they can become very toxic to organisms at high concentration levels. Other non-essential metals and metalloids, such as As, Sb, Hg, Cd, Pb, Ni, etc., are highly toxic even at low concentrations.^[1,2]

Heavy metals naturally occur in earth’s crust, however, weathering and erosion of minerals and rocks naturally rich with heavy metals can contaminate surrounding areas.^[1] In fact, soils act as a sink and a source of PTEs since they are non-biodegradable and persist in the environment for long times, ultimately altering soil properties, decreasing soil fertility and contaminating the crops.^[3,4] Moreover, anthropogenic activities such as mining, agriculture, discharge of sewage and industrial effluents, traffic and fossil fuel combustion constantly release heavy metals into the environment.^[1,3]

The mining activity is considered the major anthropogenic source of environment contamination by heavy metals. The exploitation of mineral resources changes the layout of the soil and produces huge amounts of waste that are deposited in the surrounding areas in the form of heaps and tailings. The exposure of rocks and minerals previously found in deeper layers of the soil to environmental conditions and the lack of proper monitoring and treatment of the heaps and tailings strongly increase the occurrence of acid mine drainage (AMD).^[3,5]

AMD results from the oxidation of sulfide minerals, in particular pyrite, when exposed to air and water and is one of the biggest problems associated with active or deactivated mines.^[6] The chemical reaction beyond AMD occurs as follows:^[7]



This phenomenon leads to the oxidation of sulfides and produces sulfuric acid and iron hydroxide contributing to mobilize the heavy metals from mining site or tailings to the surrounding soils and aquatic systems. Furthermore, the ADM reaction is catalyzed by microorganisms that obtain energy from the oxidation of iron and sulfur compounds, contributing to heavy metals bioavailability.^[7]

As stated before, the contamination of soils with heavy metals is a currently growing problem for environment and society since it is essential to preserve and ensure a healthy soil system for protection of groundwaters, plants and living beings that directly or indirectly depend on the ecosystems. In this framework, the potential environmental impact of two deactivated mining sites in Portugal were studied in this work. Both regions will be briefly described.

1.3. Study areas

1.3.1. Fojo waste pile of the Pejão mining complex

The Pejão coal mining complex extends along approximately 10 km from Germunde to the Fojo Paraduça area at Castelo de Paiva council.^[8] This old mine was one of the most important in the north region of Portugal and, between 1884 and 1994, coal and anthracite were heavily exploited for power generation.^[9]

The Fojo heap is one of the many mining waste piles generated by the Pejão mines and was recently affected by self-combustion after ignition by the forest fires in October of 2017. After two years of continuous combustion, the Portuguese company “*Empresa de Desenvolvimento Mineiro*” (EDM) intervened to cease the fires by remobilization of the wastes and cooling with water mixed with a cooling agent (**Figure 1**).



Figure 1 - Left: Fojo waste pile region during EDM intervention to stop the fire; Right: Waste pile after being affected by the fire.

1.3.2. Poça da Cadela mine in Regoufe

This study region is a W-Sn mining field in Regoufe, located at Arouca municipality. Its exploitation dates back to 1915, and during the World War II, it was the most important mine in the Regoufe region exploiting mainly tungsten for the allied forces war effort under British administration and investment. Nonetheless, it ceased activity in 1990 after a law decree.^[10] **Figure 2** shows some of the complex structures and residue piles nowadays.

In this mining complex, that extends through 57 ha, the most abundant ore is the wolframite but other sulfides and minerals, such as arsenopyrite, sphalerite, pyrite, bismuthinite and limonite, are also present in smaller scale.^[11]



Figure 2 – Different angles of the deactivated W-Sb Poça de Cadela mining complex and some of its residue piles in Regoufe.

1.4. Mercury toxicity and bioavailability

This work focused particularly on assessing the environmental impact of one of the most critical PTEs found in soils, mercury, due to its exceedingly bioaccumulative capacity and high toxicity for plants and organisms.^[1] In humans, it can target different organs depending on the chemical form of its species. For example, methylmercury (CH_3Hg^+) is teratogenic and can potentially affect the central nervous system, heart, kidneys and liver, while elemental mercury exposure is strongly related to respiratory diseases and lung damage.^[1,2]

Soils play an important role in the biological cycle of mercury, acting both as a sink and a source of this metal to biota, atmosphere and hydrological compartments.^[12] Mercury can be adsorbed to the soil matrix through cation exchange or by formation of stable complexes. Hg^{2+} can bind to adsorption sites in minerals surface (clays, oxides and hydroxides of aluminum, iron and manganese) or organic matter (S-containing functional groups) and potentially form organo-mineral complexes. Hg^{2+} and Hg^{2+} complexes reactivity strongly influences its availability to plants and organisms.^[4] Therefore, speciation of mercury present in soil is very important to proper assess the risk it poses to the environment and for those that benefit from it. In this context, sequential extraction procedures were used in this work for mercury speciation and fractionating in mine soils.

1.5. Mercury sequential extraction procedure – USEPA 3200

The measurement of PTEs total concentration in soil (usually using digestion procedures) is not sufficient to provide fully comprehensive data since heavy metals reactivity, bioavailability, toxicity and health risk largely depends on their chemical forms. Therefore, SEP methods to fractionate PTEs in soil samples received increased attention over the years.^[12–14]

A SEP method consists of subjecting a sample to a consecutive sequence of reagents with increasing strength to extract specific species of the desired analyte in each step of the extraction. Since the required reagent strength increases through the steps, the PTEs species extracted in the early steps of the procedure (easily extracted from the solid phase due to weak interactions) are the most concerning due to being the more labile species.^[15]

Many SEP methods have been implemented for the speciation of heavy metals. For example, the modified three-step procedure proposed by the Community Bureau of

Reference (BCR) method has been commonly used to assess the potential environmental contamination of soils with Cu, Cd, Zn, Pb, etc.^[16–18] Moreover, a method described by Shiwatana et. al. was reported to be most adequate for arsenic speciation.^[19–21]

In this work, USEPA 3200 procedure, provided by the United States Environmental Protection Agency,^[22] was used for fractioning Hg in soil samples collected from the studied deactivated mining regions. This procedure fractionates Hg into three operationally defined fractions: mobile, semi-mobile and non-mobile Hg, as shown in **Table 1**. Briefly, the mobile fraction contains mainly alkyl (i.e. CH_3Hg^+ and $\text{C}_2\text{H}_5\text{Hg}^+$) and soluble inorganic (e.g. HgCl_2) mercury species (most toxic and mobile species) that strongly contribute to Hg potential toxicity in soil. In this step, ethanol is used to dissolve the alkyl and soluble inorganic mercury species while HCl is used to remove alkyl mercury species from the soil matrix and dissolve HgO species.^[23]

In the second and third steps, the semi-mobile and non-mobile fractions, respectively, less mobile and less toxic mercury species (elemental mercury, amalgams, HgS, etc.) are extracted using acid mixtures.

Table 1 - Operationally defined fractions and related extracted species.

Operationally-defined mercury fractions	Individual mercury species
Mobile Fraction	CH_3HgCl
	$\text{CH}_3\text{CH}_2\text{HgCl}$
	HgCl_2
	$\text{Hg}(\text{OH})_2$
	$\text{Hg}(\text{NO}_3)_2$
	HgSO_4
	HgO
	Hg^{2+} complexes
Semi-mobile fraction	Hg^0
	Hg^0 - Metal (amalgam)
	Hg^{2+} complexes
Non-mobile fraction	Hg_2Cl_2 (minor)
	Hg_2Cl_2 (major)
	HgS HgSe

Several authors have successfully applied this SEP for risk assessment of mercury contaminated industrial [12,13] and mine soils [12,24]. In 2005, Fernández-Martínez *et al.* [24] applied the EPA 3200 to study the contamination of the soil of an old Asturia Hg mining site, located in Spain, that abundantly produced Hg for years. The authors found that mercury was present in soils with appreciable amounts of mobile (organic and inorganic) mercury in the soil directly in contact with the base of the vapor evacuation chimney and that Hg levels decreased with the increasing distance from this (main) source of contamination. Furthermore, they also reported that samples with finer particle size and regions subjected to more intensive weathering, such as downstream soils receiving the runoff from the chimney, have higher mercury mobility.

In another work, Frentiu *et al.* [13] evaluated the Hg contamination, using the EPA 3200 SEP, in the surrounding soils of a former chlor-alkali plant in the north-western region of Romania. The researchers found out that the semi-mobile fraction was also the dominant fraction in samples collected. The statistical analysis carried out revealed that Hg mobility in soil depends more on the pH, content of organic matter, Ca^+ , Fe^+ , Mn^+ , Cu^+ and SO_4^{2-} than natural components, such as aluminosilicates.

A particularly interesting work was conducted by Reis *et al.*, [12] in 2010, in two western regions of Portugal, the chlor-alkali plant in the Estarreja industrial complex and the deactivated Caveira sulfide mine. The authors concluded that mercury was mainly found in the semi-mobile fraction in both regions. From the statistical analysis performed in the study, they concluded that mercury had higher mobility in the industrial chlor-alkali plant soil than in the mine soil because of the higher aluminium and manganese content. By opposition, the elevated content of sulfur and organic matter in the mine soil contributed to the retention of mercury and reduction of its mobility.

Therefore, the EPA 3200 SEP showed to be suitable for the risk assessment of mercury in contaminated soils, including mine soils, by providing significant information on Hg mobility, speciation and its spatial distribution.

1.6. Mercury extraction and determination

Prior to the determination of mercury and other heavy metals by the common analytical techniques in solid samples, such as soil, it is needed to transform the samples into a solution containing the analytes. This process is usually carried out through a digestion procedure.

1.6.1. Soil sample preparation

Microwave-assisted digestion in closed vessels is nowadays one of the most commonly used procedures for soil samples analysis. Relatively to other labor intensive and tedious methods, such as hot-plate digestion, microwave-assisted digestion is faster, safer and requires less amount of sample and reagents. In addition, this technique is reported to yield more reproducible and controlled results. [25]

A variety of acids and mixtures can be used for microwave digestion of soil samples. Many methods usually use hydrofluoric acid (HF) for complete digestion of soil samples as it breaks down silicates and minerals better than other acid mixtures, such as $\text{HClO}_4/\text{HNO}_3$ and HNO_3/HCl . However, HF and HClO_4 are highly dangerous, can cause severe injuries and must be handled with extreme care [26–28].

Due to the hazardous potential of the common acid mixtures, in this work, a microwave assisted digestion procedure using *aqua regia* was adopted. This method is less aggressive than procedures that use mixtures of stronger acids, such as HF and HClO_4 , and is not intended to accomplish the total decomposition of the sample. Therefore, the obtained extracts are commonly considered to represent “pseudo-total” concentrations of the analyte in the sample. Nonetheless, recent studies reported that digestion procedures with *aqua regia* can yield, for several metals, statistically similar performance to procedures using more aggressive acid mixtures. [25,29]

1.6.2. Mercury Determination by CV-AAS

Generally speaking, mercury determination can be very challenging for several reasons, namely: (i) mercury compounds are highly volatile and during sampling and/or analysis loss of species can easily happen; (ii) sample preservation is mandatory to avoid altering Hg distribution; (iii) when dealing with trace concentrations caution with the material and samples is very important to minimize the risk of contamination from other sources, such as the reagents. [30]

The most commonly used techniques worldwide for Hg quantification are the inductively coupled plasma mass spectrometry (ICP-MS) and cold vapor atomic absorption spectrometry (CV-AAS). [30]

Although ICP-MS has proved to present very low detection limits for Hg, low sample consumption and a wide range of linearity, the memory effect is usually a problem when using this technique due to mercury adhering property. In addition, the

very high costs associated makes this technique many times not suitable for routine analysis of mercury.^[31]

The CV-AAS technique has been highly used for Hg analysis due to its high sensitivity, speed, simplicity and its lower cost relatively to other techniques, including ICP-MS. However, the disadvantages of being labor-intensive, the need for high purity of the reagents, the high sample/reagents consumption and the strong influence of transition metals in the sensitivity and reproducibility of the method are commonly reported by researchers.^[31]

1.7. Atomic absorption spectrometry

Atomic absorption spectrometry (AAS) is a commonly used technique for qualitative and quantitative analysis of more than 70 elements in concentrations ranging from parts-per-million (ppm) to parts-per-billion (ppb). Briefly, in this technique, a cloud of free gaseous atoms of the analyte is irradiated with electromagnetic radiation of a specific wavelength, produced by a light source in the ultraviolet/visible range. The measured property is the amount of radiation absorbed when the electromagnetic radiation passes through the cloud. The amount of radiation absorbed by the analyte is proportional to the concentration of the analyte in the solution prior to the nebulization step and therefore can be quantified.^[32]

1.7.1. Process of atomic absorption

An atom is made up of a nucleus orbited by a specific number of electrons in a predictable and ordered manner and is usually found in its state of lowest energy, the most stable electronic configuration (“ground state”). When the atom is stimulated, for instance by electromagnetic radiation, it can absorb sufficient energy so that an electron of an outer orbital is promoted and the electronic configuration changes to a less stable state of higher energy (“excited state”). An electron in the “excited state” tends to spontaneously return to its “ground state”, and by doing so, amongst several other manners, it can return emitting a photon with the same energy it absorbed, as exemplified in **Figure 3**. In absorption spectroscopy, the energy absorbed during the excitation of the electron is measured for analytical purposes.^[32,33]

Moreover, AAS is widely used for determination of several metals and metalloids since they possess loosely bound and readily available electrons and, thus, can be

excited by less energetic radiation of wavelengths in the visible range. The high selectivity of this technique is related to the fact that each atom has a unique specific configuration and, therefore the energy gap between the “ground state” and the “excited state” is specific for each element. [33]

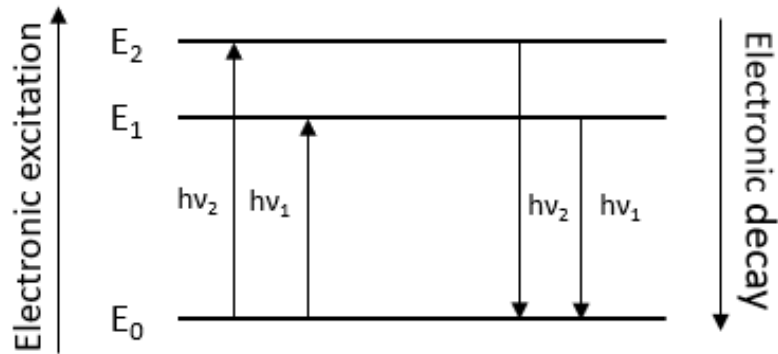


Figure 3 - State transitions by excitation or decay. (Adapted from reference 32)

1.7.2. Atomic absorption instrument

There are four main components in an atomic absorption device, as show in **Figure 4**, namely: (1) the light source, which is a source of high intensity that generates a line spectrum equal to the spectrum of the analyte; (2) an atomizer, which is a device that transforms the liquid solution into a cloud of free atoms; (3) a monochromator, that isolates the desired wavelength band to be measured and; (4) a detector, that measures and quantifies the quantity of light incided on it.

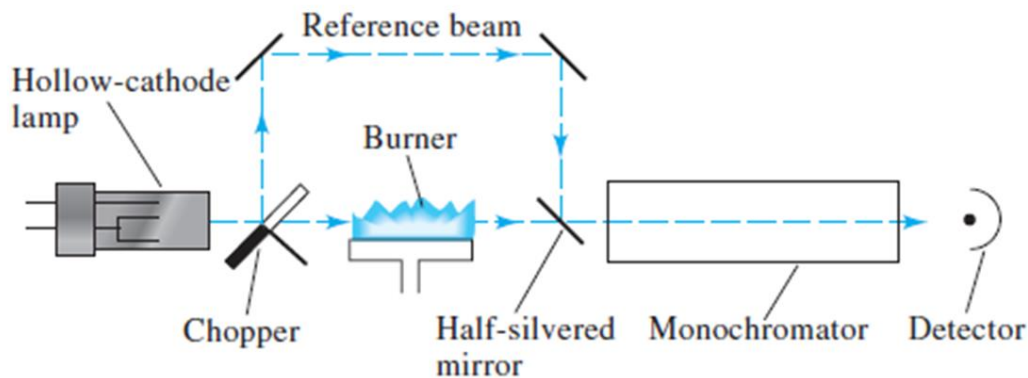


Figure 4 - Diagram of an atomic absorption spectrometer instrument (Figure from reference [32]).

The hollow cathode lamp, illustrated in **Figure 5**, is the most used light source for AAS. It consists of a glass tube containing a tungsten anode, a cylindrical cathode of a desired analyte and an inert gas (i.e. Ag or Ne) at low pressure. When a difference of potential is applied between the electrodes, the inert gas atoms ionize and accelerate towards the cathode. When the ions of the gas strike the cathode some of the metal atoms are dislodged in a process called sputtering. The dislodged metal atoms will eventually collide with the inert gas ions and through the transfer of kinetic energy change to an electronic configuration of an excited state and eventually emit at their characteristic wavelength when returning to the ground state. [32]

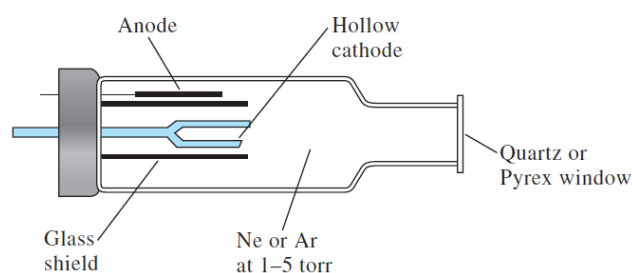


Figure 5 - Hollow cathode lamp scheme (Figure from reference [32])

The atomization process is a fundamental part of the AAS analysis. Free atoms are formed by supplying enough energy to break the chemical bonds between atoms of a molecule, commonly using a flame or an electrothermal atomizer. In a typical flame atomic absorption analysis, the solution is aspirated into a nebulizer where the liquid is

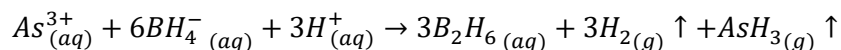
transformed into an aerosol that is sprayed into the flame. In the flame, the desolvation and vaporization of the fine droplets of the sample occurs and then the solid particles decompose into free atoms or ions for analysis. [32,33]

Although AAS is commonly used for the determination of several metals (Na⁺, Ca⁺, K⁺, etc.) [34–36] for other metals and metalloids more sensitive techniques such as hydride generation and cold vapor atomic absorption spectroscopy (HG-AAS and CV-AAS respectively) are frequently used.

1.7.3. Hydride generation technique

Some elements, such as arsenic (As), antimony (Sb) and selenium (Se), absorb radiation with wavelength below 200 nm. In this range, the absorption of radiation by the flame gases is strong and, thus, difficult the correct analysis of such elements. An alternative approach is then to take advantage of the property of some elements to form volatile hydrides. [37,38]

In this technique hydrides are generated usually by reacting the acidified sample with sodiumborohydride (NaBH₄), as shown in the equation below for As(III):

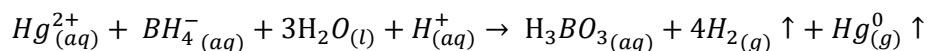


The formed hydride is carried out by an inert gas (i.e. N₂) stream to the absorption cell mounted in the burner where it will be atomized and the absorption measured normally.

The main advantages of this technique relatively to the flame AAS are the higher sensitivity obtained due to the longer residence time of the analyte in the absorption cell and that the flame gases absorption does not interfere with the measured signal. [37]

1.7.4. Mercury cold vapor technique

Continuous flow cold vapor atomic absorption spectroscopy (CV-AAS) takes advantage of the appreciable vapor pressure of Hg at room temperature. It works similarly to the HG-AAS, however, it doesn't require flame to heat the evolved Hg since it is already into its atomic form after the reduction. In the CV-AAS technique sodium borohydride (NaBH₄) or stannous chloride (SnCl₂) is used to reduce Hg⁺² into the volatile Hg⁰, as shown in the equation below: [37,39]



The evolved Hg atomic vapor is then carried by an inert gas (i.e. N₂) stream into an absorption cell, mounted in the burner, as illustrated in **Figure 6**, where the electromagnetic radiation will pass, and the absorption will be measured normally as in any other AAS technique. Similarly, to the HG-AAS one of the advantages of this technique is its increased sensitivity relatively to flame AAS (about 100 times higher) due to the longer residence time of the chemical vapor in the absorption cell. [37]

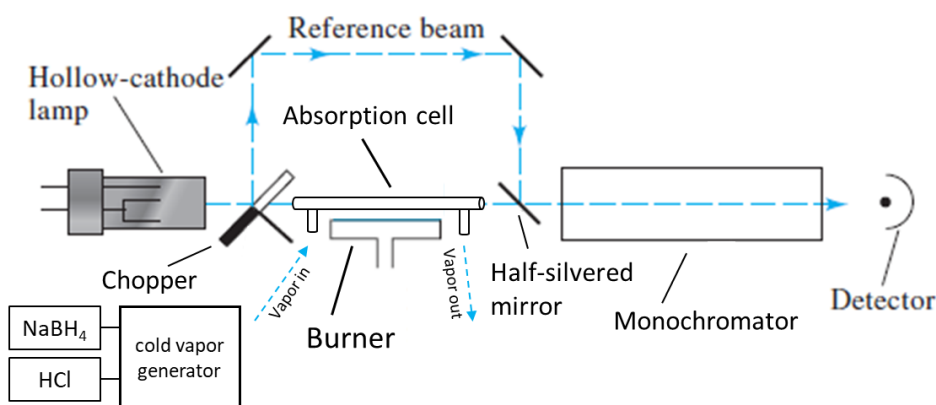


Figure 6 - Diagram of AAS instrument setup for CV-AAS analysis (Figure adapted from reference [32]).

1.8. Objectives

As stated before, this work aims to study the contamination and dissemination of mercury species in the surrounding area of two deactivated mines, the Pejão mining complex, located in Castelo de Paiva, and the Poça da Cadela W-Sb mine, located in Regoufe, originated from residues produced by them to provide information about the risks imposed by mercury to the environment and potentially to human health.

For that, the methodology consisted in the determination of the pseudo-total concentration of mercury and its comparison with reference and background values to ascertain the extent of the soil contamination. The samples were subjected to a sequential extraction procedure (SEP) for fractioning of the contaminant to assess the risk it poses to the environment and to organisms according to its bioavailability.

2. Materials and methods

2.1. Safety measures

The following safety measures were adopted in this work to properly handle contaminated soil samples, mercury and other heavy metal solutions and contaminated material:

- In addition to appropriate eye protection gear, gloves made of nitrile (or other appropriate material) were required to properly protect against organomercury compounds.
- In case of direct contact with any mercury solution, gloves were immediately removed, disposed properly and replaced by new gloves.
- Gloves, pipette tips, etc., which might have come in contact with mercury containing compounds were disposed in a dedicated waste bin fitted with a tight lid. The waste bins were kept in the hood or other ventilated area.
- In the event of a spill, the area was kept well ventilated, the liquid absorbed on paper towels and discarded in a designated waste bin.

For handling of *aqua regia*, the following safety measures were adopted:

- All procedures involving *aqua regia* were realized in a fume hood, as dissolving metals in *aqua regia* releases toxic gases.
- When preparing the *aqua regia* solution the nitric acid was always added to the hydrochloric acid slowly.

2.2. Soil sampling and processing

Twenty-five samples were collected from sampling sites in the Fojo coal waste pile region, according to the distribution presented in **Figure 7**, namely: ten samples of mining residues affected by combustion (“escombreira ardida”, EA), five samples of mining residues unaffected by combustion (“escombreira não ardida”, ENA), five

samples of soil from the woods upstream to the waste pile ("background", B) and five samples of soil from a downstream region relatively to the waste pile ("solo a jusante", SJ).

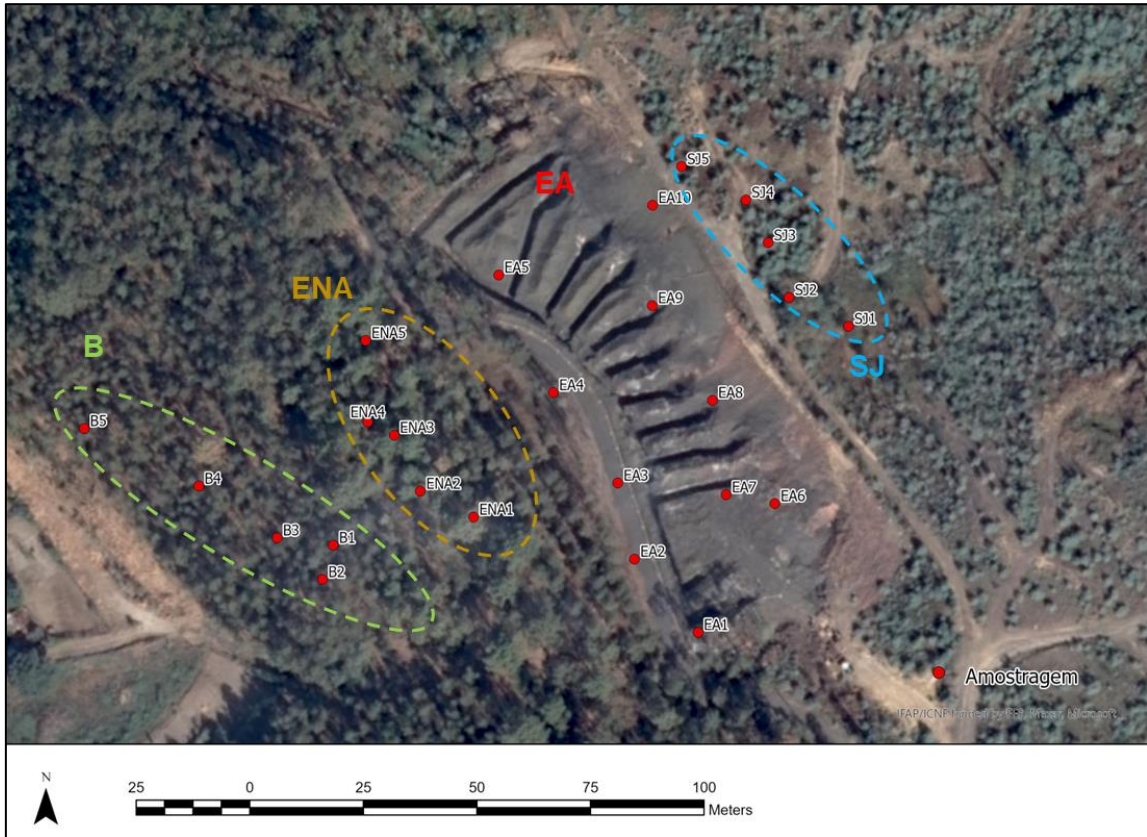


Figure 7 - Sample distribution map in Fojo region.

In the Regoufe deactivated mine, twenty samples were collected from different sampling sites according to the distribution shown at **Figure 8**. The samples were collected close to the mine entrances, along the ore processing line, at the waste piles (of both thin and bulk materials) and along the mine drainage line.

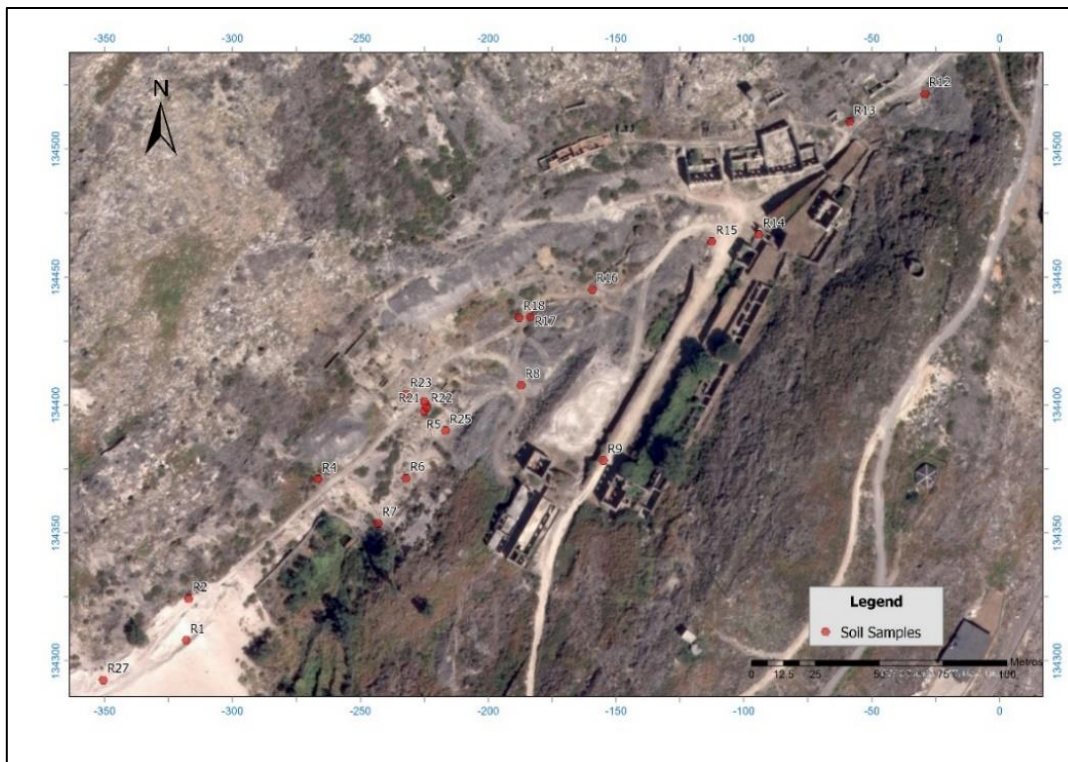


Figure 8 - Sample distribution map in Regoufe region.

All samples used in this work were collected and supplied by the Department of Geosciences, Environment and Spatial Plannings of Porto University. Based on the researcher's previous knowledge of the region a judgmental sampling was performed on both regions. The collected samples were dried ($< 60^{\circ}\text{C}$) and sieved through a 2 mm mesh. Working samples of different mass for the digestion (~ 0.25 g) and sequential extraction procedures analysis (~ 1.0 g) were obtained using the coning and quartering subsampling method, used to homogenize the samples by pouring and mixing the sample so that it takes on a conical shape, flattening it out, dividing it into four quarters and discarding two opposite quarters repeating the process with the remaining sample until the desired sample size is reached.^[40] Furthermore, all samples were kept in the refrigerator until utilization.

2.3. Materials, instruments, reagents and solvents

2.3.1. Common labware

The materials used in this work were:

- Ergonomic High-Performance micropipettes (VWR; 100-1000 μL , 20-200 μL , 1-5 mL and 1-10 mL)

- Single use syringes (ECOJET; 10 mL and 20 mL)
- Non-sterile nylon syringe filters (Branchia; 0.45 μm pore)
- Qualitative filter paper (Whatman; grade 5)
- Centrifuge tubes (Astik's; 15 mL and 50 mL)
- Regular use laboratory glassware material (volumetric flasks, graduated flasks, beakers, etc.)

To perform this work, all laboratory-ware in contact with samples or chemical solutions prepared were made of borosilicate glass or polypropylene (centrifuge tubes, etc.). Prior to its reutilization, the materials were decontaminated by being soaked in HNO_3 10% (w/v) overnight and later rinsed abundantly with deionized water and pure water. New plastic and glass materials were used without prior decontamination.

2.3.2. Common lab instruments

The common instruments used in this work were:

- Pro-Analytical centrifuge (Centurion Scientific)
- Vortex stirrer (LBX instruments; V05 series)
- Analytical balance (A&D; GR-202)
- Hot plate magnetic stirrer (IKA; C-MAG HS 7)
- Ultrasonic bath (Bandelin Sonorex; Digitec DT 100 H)

2.3.3. Reagents and solvents

All reagents and solvents used, shown in **Table 2**, were of analytical grade adequate to accurate trace metal determination by atomic spectrophotometric techniques and were used without further purification.

Table 2 - Reagents and solvents used.

Reagent	Purity and/or Quality	Company
Sodium borohydride	99%, ReagentPlus	Sigma-aldrich
Sodium borohydride	99%	Acros organics
Sodium hydroxide	≥ 98%, Analytical grade	Sigma-aldrich
Ethanol, absolute	≥ 99.8%, HPLC grade	Fisher-chemical
Hydrochloric acid	37% (w/v), Laboratory grade	Fisher-chemical
Nitric acid	69% (w/v), ACS grade	Fisher-chemical
Mercury standard solution	certified solution	Thermo Scientific

After using the sodium borohydride, the solid was purged with a nitrogen stream, the bottle covered with parafilm paper and stored inside the vacuum desiccator to preserve the reagent.

All aqueous solutions used in this work were prepared using water purified with a Milli-Q purification system (resistivity ≥ 18 MΩ.cm).

2.4. Soil sample digestion with *aqua regia*

For each collected sample, the *aqua regia* soluble Hg (or Hg pseudo total concentration) was determined by a microwave-assisted digestion procedure, based on protocols described in ISO 12914^[41] and USEPA 3051A^[42]. This procedure was executed controlling the power program (instead of temperature ramp, which is not available for our microwave system), as shown in **Table 3**. The microwave dissolution program was based on published literature^[43] reporting soil samples digestion and aiming to maintain the temperature inside vessels around 175 °C for 20 min (as reported in USEPA 3051A).

Table 3 - Operating condition for microwave digestion procedure.

Step	Power (W)	Hold time (min)
1	400	2
2	600	2
3	700	20
4	0	10

To perform the soil digestion, only a small amount of sample was used to minimize the formation of gases and avoid the rupture of the safety membrane due to excessive pressure inside the vessel. Therefore, about 0.25 g of homogenized soil sub-samples

were weighted to 100 mL PTFE vessels and placed in a fume hood. Then, 6.0 mL of concentrated HCl and 2.0 mL of concentrated HNO₃ were added to the pre-cleaned digestion vessels.

Aqua regia was prepared immediately prior to using as storing it for long periods of time leads to a loss of effectiveness of the mixture due to oxidation of its reactive components. Furthermore, solutions of premixed combination of acids result in chlorine gas buildup, as well as of other gases.

Then the vessels were placed inside the microwave rotor, sealed tight using the multifunctional lid of the system, that serves as rack for up to 6 vessels and protection shield during reaction, and finally submitted to the microwave dissolution in an Anton Paar MULTIWAVE 1000W microwave oven (**Figure 9**).

The experiments performed using the power program shown in **Table 3** revealed that when maximum power of 700 W was applied (step 3), the monitored temperature inside vessels was around 185 °C

After digestion and cooling of the samples, the final solutions were filtered through Whatman filter papers, transferred into 25 mL or 50 mL volumetric flasks, and the volume made up with pure water prior to analysis by CVAAS.



Figure 9 - Microwave-assisted digestion system consisting of oven, rotor and vessels.

After each sample digestion, and before reutilizing the vessels, a decontamination procedure was applied. To each vessel, 6.0 mL of a 1:2 HNO₃:H₂O solution was added,

and after proper sealing, heated in the microwave oven under the conditions shown in **Table 4**.

Table 4 - Decontamination procedure operating conditions.

Step	Power (W)	Hold time (min)
1	600	5
2	800	10
3	0	10

2.5. Mercury sequential extraction procedure

In this work, the USEPA 3200^[22] procedure was adopted. It is a three-step standard sequential extraction procedure (SEP) proposed by the Environmental Protection Agency (EPA) in which mercury species are fractionated in three parts: mobile mercury, semi-mobile mercury and non-mobile mercury.

2.5.1. Extraction solutions

To perform the SEP procedure in collected soil samples, the following solutions were used:

- (Step 1) 2.0% (v/v) HCl + 10% (v/v) ethanol extraction solution, prepared by direct dilution of concentrated HCl and ethanol in pure water.
- (Step 2) 1:2 (v/v) HNO₃:H₂O extraction solution, prepared by combining 1 part of concentrated HNO₃ with 2 parts of pure water.
- (Step 3) 1:6:7 (v/v/v) HCl:HNO₃:H₂O, prepared by combining 1 part of concentrated HCl, 6 parts of concentrated HNO₃ with 7 parts of pure water.

2.5.2. Extraction of mobile mercury – Step 1

To a 15 mL centrifuge tube, 1.0 ± 0.5 g of the soil sample was weighted and subjected to 2.50 mL of a mixture of 2% HCl and 10% ethanol. The sample was agitated in a vortex and centrifuged (3200 rpm for 10 min) to evaluate the pH of the supernatant. When necessary, the pH was adjusted by adding concentrated HCl drop-wise until the value was between 1.5 and 3.0. The samples were placed again in the vortex and then

heated in an ultrasound bath for 7 min at 60 ± 2 °C, as schematically represented in (Figure 10).

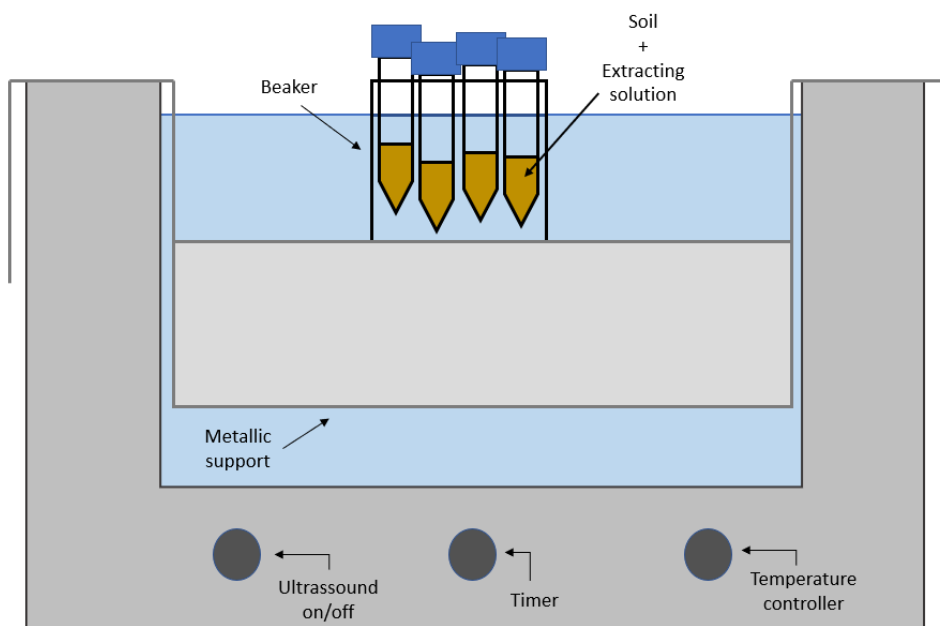


Figure 10 - Scheme of the ultrasound bath used in the first extraction step.

After the extraction, the supernatant was separated by centrifugation at 3200 rpm for 10 minutes. The extraction process was repeated two more times without further pH test and adjustment. Finally, the sample residue was washed with 2.50 mL of pure water, vortexed for 1 min, centrifugated and the water rinse combined with the extracts. The final solution was filtered using a $0.45 \mu\text{m}$ nylon membrane syringe filter, acidified with concentrated HCl (to ensure a minimum final HCl concentration of 5%) and diluted with pure water to a final volume of 20.0, 25.0 or 50.0 mL before analysis by CV-AAS.

2.5.3. Extraction of semi-mobile mercury – Step 2

Before proceeding to the extraction of the semi-mobile species, the presence of chloride ions at the residue was evaluated since Cl^- can promote the solubility of non-mobile mercury species (e.g., HgS) into the semi-mobile extract solution which must be avoided. All samples revealed the presence of chloride ions, and, therefore, the sample residues were washed with 5 mL of pure water until the addition of $0.1 \text{ mol.L}^{-1} \text{ AgNO}_3$ causes no turbidity^[24]. This procedure, however, was not applied more than three times^[24].

For extraction of semi-mobile species, 5.00 mL of 1:2 (v/v) HNO₃:H₂O solution was added to the residue of the previous step and mixed for 1 min using the vortex. The mixture was heated to 95 ± 2 °C for 20 min in a water bath (**Figure 11**). To avoid losses of volatile mercury species, the cap tubes were loosely tightened during the heating step. After cooling to room temperature, samples were centrifuged (3200 rpm, 20 min) and the supernatant collected to another recipient. The extraction procedure was repeated once more, and the supernatants combined. Finally, the remaining soil was rinsed with 5.00 mL of pure water, vortexed for 1 min, centrifuged at 3200 rpm for 20 min and the supernatant combined with the extracts. The final solution was filtered, acidified with concentrated HCl (final concentration of 5%) and diluted with pure water to a final volume of 20.0, 25.0 or 50.0 mL before analysis by CV-AAS.

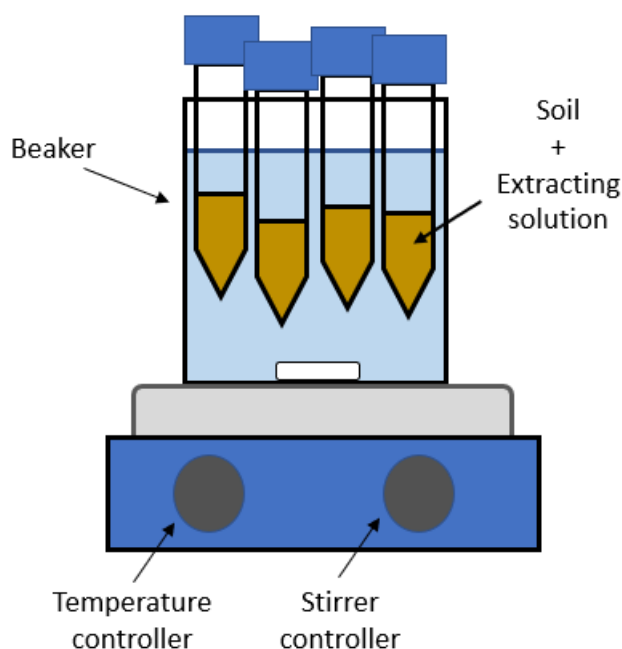


Figure 11 - Representative scheme of the water bath system used in the second extraction step.

2.5.4. Extraction of non-mobile mercury – Step 3

A procedure similar to the one used in the previous step was applied to the samples' residues of step 2. Briefly, 5.00 mL of 1:6:7 (v/v/v) HCl:HNO₃:H₂O solution was added. The samples were vortexed for 1 min and then heated in a water bath to 95 ± 2 °C for 20 min similarly to step (see **Figure 11**). To avoid losses of volatile mercury species, the cap tubes were loosely tightened during the heating step. After cooling to

room temperature, the samples were centrifuged (3200 rpm, 20 min) and the supernatant collected to another recipient. The extraction repeated once more and the supernatants combined. Finally, the remaining soil was rinsed with 5.0 mL of pure water, vortexed for 1 min, centrifuged at 3200 rpm for 20 min and the supernatant combined with the extracts. The final solution was filtered, acidified with concentrated HCl (minimum concentration of HCl equal to 5% v/v) and diluted with pure water to a final volume of 20.0, 25.0 or 50.0 mL before analysis by CV-AAS.

2.6. Mercury analysis by Cold Vapor Atomic Absorption Spectrometry (CV-AAS)

2.6.1 Instrumentation

CV-AAS analysis was performed using a Thermo Scientific iCE 3000 Series double-beam Atomic Absorption Spectrometer combined with the VP100 accessory, a continuous flow vapor generation (hydride) system. The combined system is shown in **Figure 12**. The AAS system and the VP100 were both fully controlled by the Thermo Scientific software SOLAAR.

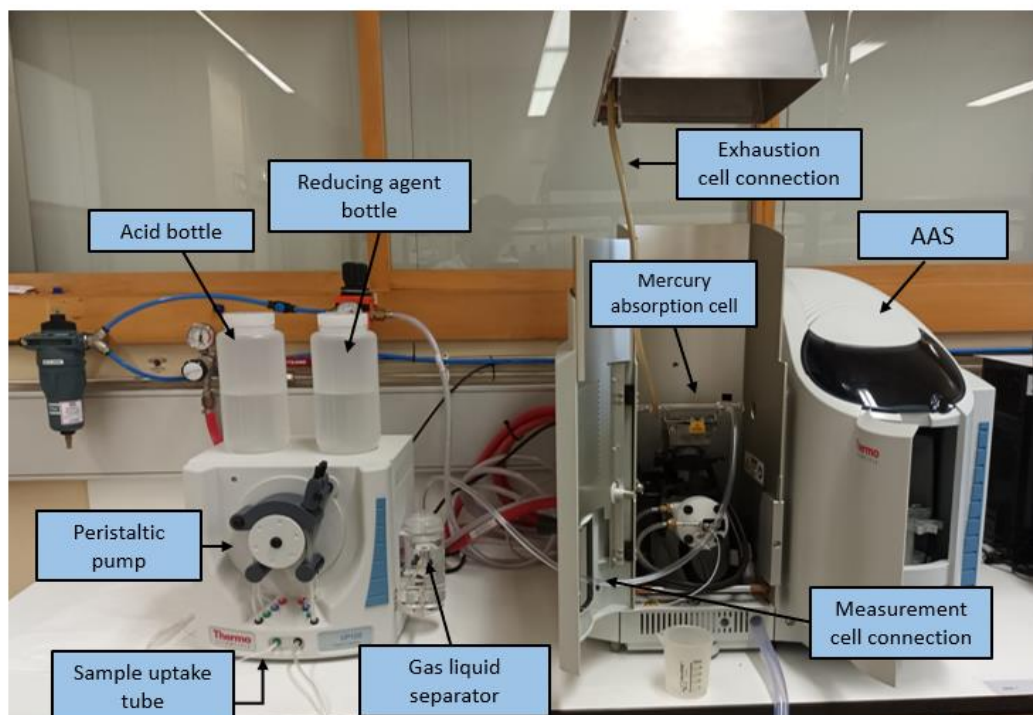


Figure 12 - VP100 (left) and atomic absorption *spectrometer* (right) used for CV-AAS measurements.

For Hg measurement by CV-AAS a specific absorption cell, shown in **Figure 13**, was used. The volatile mercury is carried by a stream of nitrogen from the reaction

chamber of the VP100 equipment to the cell mounted in line with the path of the radiation for the absorption measurement. This cell design offers improved sensitivity and precision compared to the common “T” cell used for hydride analysis.

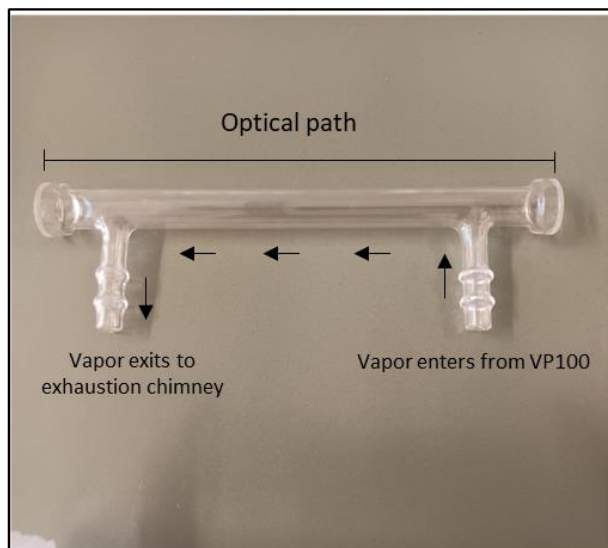


Figure 13 - Absorption cell used in this work for determination of mercury.

2.6.2. Solutions for Cold Vapor/Hydride generation

Diluted hydrochloric acid and sodium borohydride were selected for Hg cold vapor generation at the VP100 continuous flow vapor generator system.

Acid solution

A 10% (w/v) hydrochloric acid solution was used and was prepared by direct dilution of concentrated hydrochloric acid (37% w/v) with pure water.

Reducing agent solution

A 1% (w/v) sodium borohydride solution was used as reducing agent. Since this compound may react vigorously with water, it was stabilized in 0.5% (w/v) sodium hydroxide solution. This solution usually loses strength in three to four days even if kept stored under 4 °C. Thus, to guarantee the best reaction performance, fresh solutions were prepared immediately prior to the analysis.

The intended amount of solution was prepared by first weighting an appropriate mass of NaOH to a graduated flask followed by its dissolution in water. Then, the proper amount of NaBH₄ was added and the final volume made up with pure water.

2.6.3 Operation conditions

After the optimization of the experimental conditions the operating parameters shown in **Table 5** were adopted for the Hg measurements.

Table 5 - Operating conditions of the CV-AAS system.

AAS and VP100 operating conditions	
Slit width	0.5 nm
Burner height	15 mm
Hollow lamp wavelength (Hg)	257.3 nm
Lamp current/voltage	75 %/ 6 V
Signal measurement	Transient Height
Signal type	Background correction
Total measurement time	100 s
Sample aspiration time	25 s
Carrier gas flow	100 mL.min ⁻¹
Pump speed	40 rpm
Sample uptake rate	7.5 mL.min ⁻¹
Reducing agent uptake rate	1.6 mL.min ⁻¹
Acid uptake rate	0.7 mL.min ⁻¹

In this method, deuterium background correction was used. Thus, to perform background correction and eliminate any interference from atoms that absorb light at the same wavelength as mercury a deuterium lamp was used. The signal obtained by the deuterium lamp was automatically subtracted from the value obtained with the hollow lamp by the AAS software.

2.6.4 Calibration curve for mercury and analytical parameters

2.6.4.1. Hg solutions preparation and Hg determination

For the quantification of Hg, calibration curve method was used. To build the calibration curve, Hg standard solutions of 2.00, 5.00, 10.0, 15.0 and 20.0 µg L⁻¹ were

prepared from a stock solution ($C = 1004 \pm 7 \text{ mg.L}^{-1}$) by adding to different volumetric flasks appropriate aliquots of a 2.00 mg.L^{-1} intermediate solution and making up the volumes with 10% w/v HCl.

The sampling time was particularly important in this work due to the limited amount of sample solution. In CVAAS technique, the signal is continuously measured during 100 s. If the sample was continuously aspirated during the measurement, it would require a large sample volume (of about 15-20 mL) per measurement. However, a final solution volume of ~10 mL was obtained after the extraction/digestion of samples (before filtration and acidification). Thus, to avoid diluting the samples extracts and to allow duplicate measurements of the same sample solution, the sample aspirating time was reduced in this work although not compromising detection sensitivity.

For Hg measurement in this work, samples were aspirated for 25 s consuming only ~4 mL of the sample. Furthermore, a resting time of 10 s before starting sampling aspiration was implemented to minimize operator errors and to increase reproducibility of results. Considering the 100 s of Hg measurement, during the first 10 s no sample was aspirated, from 10 s to 35 s the sample was aspirated and from 35 s to end of the measurement no sample was aspirated (**Figure 14**).

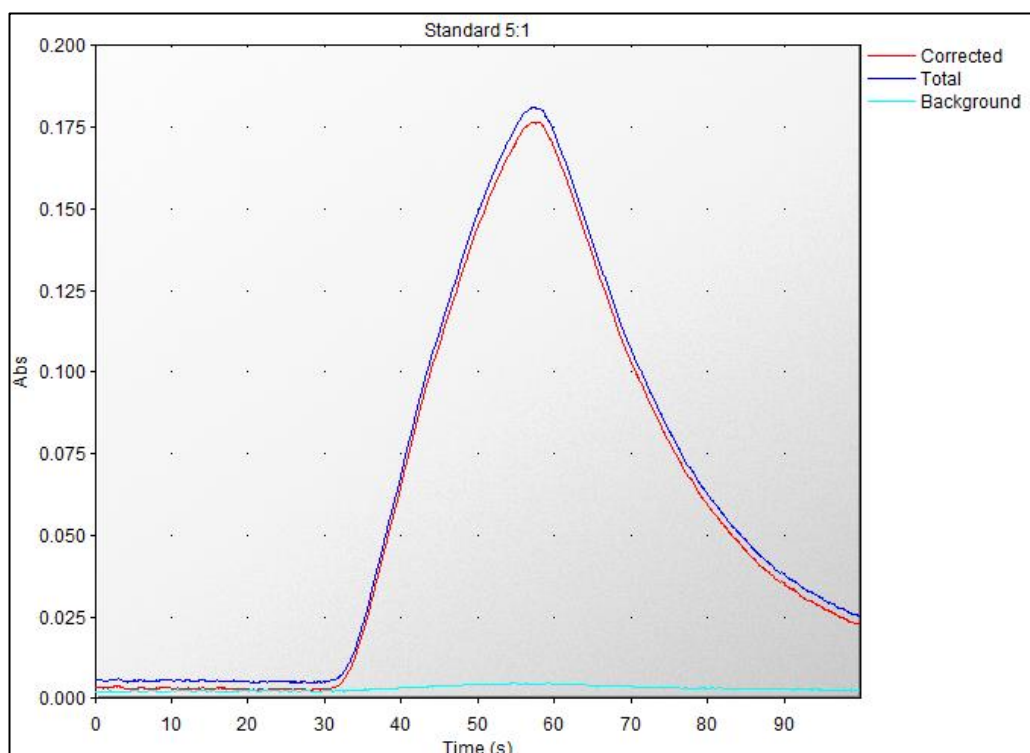


Figure 14 - Typical graphical representation of absorbance versus time obtained for a $20.0 \text{ }\mu\text{g.L}^{-1}$ Hg solution. The total measurement time was 100 s.

After each Hg measurement, a 10 % (w/v) hydrochloric acid solution was aspirated to clean the sampling tube and the mercury cell and thus minimizing the occurrence of “memory effects” between measurements.

2.6.4.2. Analytical parameters

Sensitivity

In atomic absorption spectrometry it is defined as the concentration, in ppm, of an aqueous solution of an element that gives an absorbance of 0.0044 (equal to the absorption of 1% of the transmitted radiation).

Sensitivity for mercury analysis was checked by aspirating a solution that gave an absorbance reading of about 0.1. After adjusting the equipment parameters for better sensitivity, the concentration of mercury to give an absorbance of 0.0044 can be easily estimated.

Linearity

The linearity of a method is its ability to generate signals directly proportional to the analyte concentration within a specific working range. The simplest way to observe the linearity of a method is through the graphical representation of the analytical signal vs. the analyte concentration or substance quantity.

Analysis of the linear correlation factor is commonly used to verify the linearity of a calibration curve but there are several other statistical methods that can be used to evaluate linearity. In this work, the linearity was evaluated using statistical model described in ISO 8466-1 (Mandel test)^[44]. From a set of ordered pairs, the linear calibration function and the nonlinear calibration function are obtained and the respective residual variance, $S^2_{y/x}$ and $S^2_{y^2}$, are calculated using equations 1 and 2 respectively.

$$S^2_{y/x} = \frac{\sum_{i=1}^n (y_i - (mC_i + b))^2}{n-2} \text{ (Eq. 1)}$$

$$S^2_{y^2} = \frac{\sum_{i=1}^n (y_i - (m_2 C_i^2 + mC_i + b))^2}{n-3} \text{ (Eq. 2)}$$

The difference of the variances (DS^2) is calculated by the following equation:

$$DS^2 = (N - 2)S_{y/x}^2 - (N - 3)S_{y^2}^2 \text{ (Eq. 3)}$$

The test value is then calculated by the expression:

$$VT = \frac{DS^2}{s_{y^2}^2} \text{ (Eq. 4)}$$

Finally, the test result is compared with the tabulated Fischer value:

- If $VT \leq F$: the calibration function is linear of 1st degree.
- If $VT > F$: the calibration function is not linear. The working range must be reduced so that the function becomes linear, or a function of higher degree must be used.

Limit of detection

The limit of detection (LOD) of an analytical method is defined as the smallest quantity of an analyte in a sample that can be identified and is significantly different from the blank but cannot be accurately nor precisely quantified. There are different methodologies for determining the LOD. In this work, the LOD was obtained from the calibration curve according to the equation^[45,46]:

$$LOD = \frac{3.3 s_b}{m} \text{ (Eq. 5)}$$

where s_b is the standard deviation of the intercept and m is the slope of the calibration curve.

Limit of quantification

The limit of quantification (LOQ) is the smallest quantity of an analyte in a sample that may be quantified with acceptable precision and accuracy. Like for the LOD, there are different methodologies to obtain the LOQ of an analytical method. In this work, it was estimated by the equation:^[45,46]

$$LOQ = \frac{10 s_b}{m} \text{ (Eq. 6)}$$

where s_b is the standard deviation of the intercept and m is the slope of the calibration curve.

Precision of the analytical result

The uncertainty of the measurement expresses the lack of knowledge about the real value and judges the adequacy of a result for its intended purpose to verify its consistency with other similar results.^[45] In this work, to estimate the uncertainty associated to Hg concentration in mine soil samples (*aqua regia* extractable Hg and fractioned Hg after the SEP), some duplicate samples were randomly selected, using a table of random numbers, and submitted to the same experimental conditions to evaluate the variability. Although working with all samples in duplicate would be advisable, this approach would be too laborious and time-consuming. Thus, some samples per region were randomly selected to perform assays with duplicates. It is important to mention that the precision obtained by this approach englobes all sources of error from the whole extraction procedure (and not only precision of the analytical method) and the obtained value was adopted as representative of all analyzed samples of the same region.

The precision value was obtained through the following equation:

$$s = \sqrt{\frac{\frac{(y_1 - y'_1)^2}{2} + \frac{(y_2 - y'_2)^2}{2} + \dots + \frac{(y_n - y'_n)^2}{2}}{n}} \quad (\text{Eq. 7})$$

where y_n and y'_n are the values obtained for a sample and it's replicate and n the number of samples replicated.

3. Results and discussion

In this chapter, the results will be presented and discussed chronologically, starting by the optimization of the experimental conditions for mercury analysis by CV-AAS, followed by discussion of Hg concentration obtained from the digestion of the mine soil samples (total Hg content) and after application of the sequential extraction procedure (SEP), first for the Fojo waste piles and then for the Regoufe mine.

3.1. Optimization of experimental conditions for cold vapor/hydride generation

As stated before, in this work, an automatic continuous flow vapor generator system, the VP100 accessory, was used for hydride/cold vapor generation. Therefore, the first part of this work was focused on the optimization of the experimental conditions of the VP100 system taking into consideration three important factors that strongly affect the sensitivity of the CV/HG-AAS technique, namely:

- Carrier gas (N₂) flow;
- Pump speed;
- Selection of the proper reagents for hydride/cold vapor generation and their concentrations.

The optimization of these parameters was mainly based in published literature, the manufacturer methods manual^[37] and also on preliminary experiments performed to improve the sensitivity of trace metal analysis.

3.1.2. Chemical variables optimization

Before the optimization of the instrument variables the chemical parameters had to be established since the efficiency of generation of the volatile hydride species and mercury cold vapor is highly influenced by the acidity of the medium where the reaction is performed and the concentration of the reducing agent.^[47] In this work, Hg was the focus of analysis, however, in the context of the research project this study is part of the reagents used were chosen so that both CV-AAS and HG-AAS could be easily performed using the same reagents.

Relatively to the reducing agent, it is recommended in the manufacturer methods manual^[37] to use a sodium borohydride (NaBH_4) solution with a concentration between 0.5 and 1% (w/v). It is reported in the literature that low concentrations of NaBH_4 (< 0.5%) may not be enough to carry out the reaction for hydride generation (decreasing the sensitivity) while high concentrations of NaBH_4 (> 1.5%) can cause noisy backgrounds and higher variability due to excessive water vapor in the atomization cell, decreasing the sensitivity.^[38]

In this work, although lower concentrations of NaBH_4 (between 0.1 and 0.5%) have been reported to yield a high efficacy of mercury cold vapor generation^[48], a 1% (w/v) NaBH_4 solution was used since it is compatible with both, hydride (and cold vapor generation, allowing the simple detection of several metals (As, Sb, Hg, etc.) in the same soil sample extract.

Moreover, since NaBH_4 is only stable in basic solution and is readily decomposed in acidic aqueous solution, the reducing agent solution was prepared in a 0.5% (m/v) sodium hydroxide (NaOH) solution as recommended in the manufacturer methods manual.

Relatively to the acid reagent, hydrochloric acid is commonly used.^[38] It is recommended in the manufacturer methods manual^[37] to use an hydrochloric acid solution with a minimum concentration of 5% v/v.^[37] In addition, the literature showed that within the HCl concentration range of 5–30% there was no significant variation of the Hg signal intensity.^[38,49] In this work, a 10% v/v HCl solution was used for trace metal analysis using HG/CV-AAS technique.

3.1.1. VP100 instrument variables optimization

In this work, it was very important to reduce sample consumption since from the procedures of soil digestion and fractioning of mercury applied in this work, it is obtained a sample volume of about 10 mL prior to solution acidification and filtering. Thus, the carrier gas (N_2) flow and the pump speed of the VP100 equipment were first optimized to find the optimal balance between speed, sensitivity and also sample volume consumed per measurement.

Relatively to the carrier gas flow, low flow rates (< 100 $\text{mL}\cdot\text{min}^{-1}$) do not carry the vapor formed to the absorption cell properly and increases the stabilization time while high flow rates (> 300 $\text{mL}\cdot\text{min}^{-1}$) can cause the dilution of the evolved species and/or

decreases the analyte residence time in the absorption cell, affecting the detection sensitivity.^[33,47]

Relatively to the pump speed, it is easily understood that low pump speeds (10 – 20 rpm) affects the extension of the hydride/cold vapor reaction since it introduces insufficient quantity of reagents for the reaction occur, increasing the stabilization time. Although an increase of the pump speed increases the analytical sensitivity as more reagents reach the reaction chamber, high pump speeds (> 40 rpm) greatly increases the consumption of reagents and sample and can lead to liquid accumulation at the reaction chamber and/or tubes that can alter the regular vapor flow.^[33,49]

The manufacturer methods manual recommends a carrier gas flow between 50 - 150 mL.min⁻¹ and a pump speed between 30 - 40 rpm for Hg analysis by CV-AAS using VP100 accessory^[37]. Thus, preliminary assays were performed where the aforementioned parameters were independently varied along the recommended intervals as shown in **Table 6**.

Table 6 - Preliminary assays results for instrumental optimization.

Gas Flow	Pump speed	Absorbance
50		0.034
100	40	0.038
150		0.035
	30	0.032
100	40	0.038
	50	0.035

Considering the recommendations of the manufacturer, the literature consulted about trace metal detection by hydride generation/cold vapor analysis and the results of the preliminary assays (**Table 6**), a gas flow rate of 100 mL.min⁻¹ and a pump speed of 40 rpm was selected in this work for Hg analysis aiming to guarantee a high detection sensitivity, a short stabilization time while reducing the consumption of reagents and samples.

3.2. Hg measurement and calibration curve for Hg quantification

As stated before, the total measurement time defined for this work is of 100 s and thus, the procedure was optimized to reduce the consumption of the sample. Therefore, the protocol for Hg measurement in samples and standard solutions started with a resting time of 10 s, following by the aspiration of the solution for 25 s (corresponding to a sample volume of only ~4 mL) and another resting time of 65 s.

The obtained graphic profile of absorbance versus time had a peak shape, as observed in **Figure 14**. The peak maximum corresponds to the higher quantity of mercury volatile species accumulated within the absorption cell. Both, peak height and the area under the peak, can be used for quantification purposes.

In this work, a calibration curve was obtained daily for Hg analysis by measuring five mercury standard solutions with concentrations in the range from 2.00 to 20.0 $\mu\text{g}\cdot\text{L}^{-1}$ by plotting the measured peak height versus the corresponding Hg concentration. The peak height was used instead of the peak area as analytical signal since the latter approach was more affected by operator errors that altered the integration region, such as the precise start and/or end of sample aspiration. On the other hand, the peak height value was not affected by such errors, providing more reliable results and repeatability.

For example, **Figure 15** and **Figure 16** show typical calibration curves obtained for Hg analysis in soil extracts by CV-AAS using the peak height and the area under the peak, respectively. As can be seen, higher linearity of the calibration curve was achieved when the analytical signal of the analyzed standards used to create the curve was the peak height instead of the peak area.

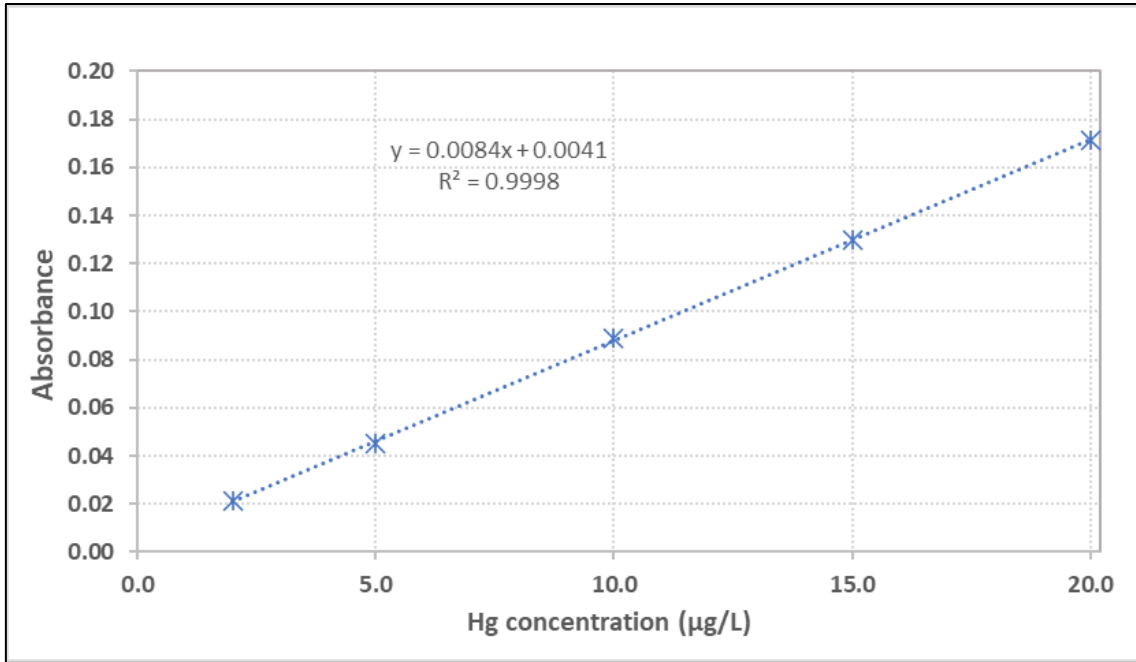


Figure 15 - Typical calibration curve obtained for the determination of mercury by using peak height as analytical signal. Standard solutions of 2.00, 5.00, 10.0, 15.0 and 20.0 mg.kg⁻¹ were used.

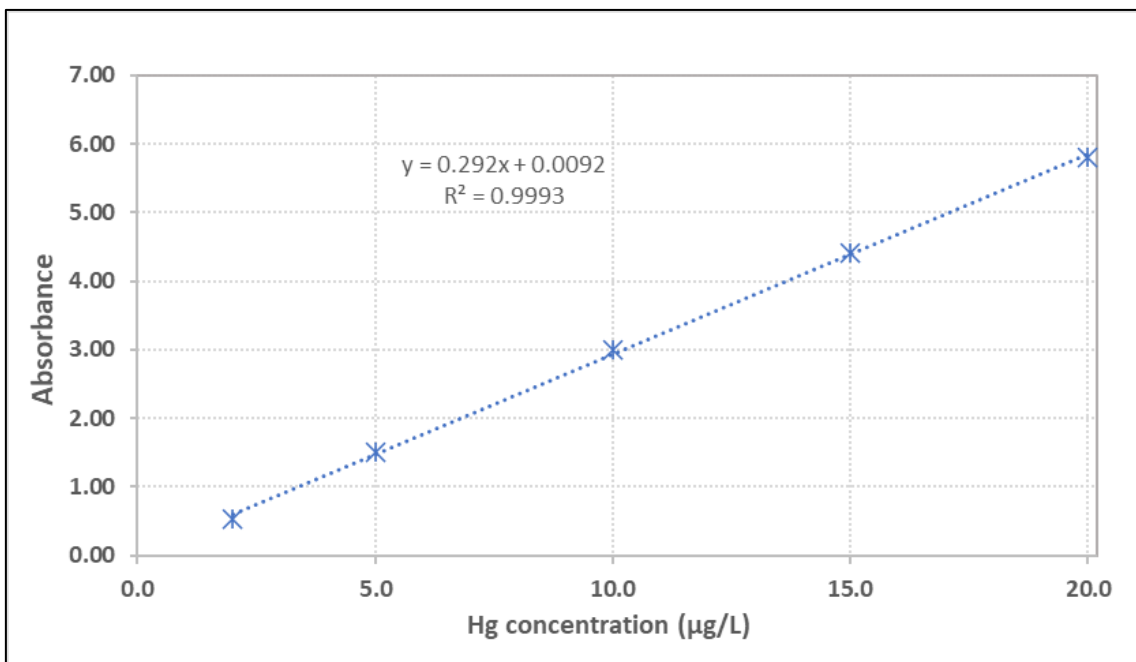


Figure 16 - Typical calibration curve obtained for the determination of mercury by using peak area as analytical signal. Standard solutions of 2.00, 5.00, 10.0, 15.0 and 20.0 mg.kg⁻¹ were used.

Considering the calibration curve shown in **Figure 15** as representative of the employed CV-AAS method for Hg trace analysis, the obtained analytical parameters are summarized in **Table 77**. The parameters were calculated as described in section

2.6.4.2. Analytical parameters and using the statistical parameters of the calibration curve shown in **Figure 15**.

Table 7 - Calculated analytical parameters

Analytical parameter	Statistical parameters	Calculated values/decisions
LOD	$s_b = 0.0009$	0.3 µg/L
LOQ	$s_b = 0.0009$	1.0 µg/L
Sensitivity	$Abs(10 \mu\text{g}\cdot\text{L}^{-1}) = 0.089$	0.5 µg/L
Linearity	$VT = -2.00; F_{\text{tab}}(0.99,1,2) = 34.12$	Linear

Linearity

The Mandel test was used to verify the linearity of the calibration curve. Using the equations and the procedure explained in section **2.6.4.2. Analytical parameters** the linear and non-linear calibration functions, the residual variances ($s_{y/x}$ e s_y^2), the difference between variances (DS^2) and the test value (VT) were obtained. Then the test value was compared to the tabulated F to verify the linearity and since the $VT < F_{\text{tab}}(0.99,1,2)$ the calibration function is linear.

Sensitivity

According to the methods manual a solution of $6 \mu\text{g}\cdot\text{L}^{-1}$ gives an absorbance signal of about 0.1. After preliminary assays a standard solution of $10.0 \mu\text{g}\cdot\text{L}^{-1}$ was aspirated to estimate the concentration of mercury to obtain an absorbance of 0.0044 using the equation bellow.

$$\text{Sensitivity} = \frac{0.0044 \times C_{\text{sol}(\sim 0.1 \text{ abs})}}{\text{Absorbance}} = \frac{0.0044 \times 10 \mu\text{g}\cdot\text{L}^{-1}}{0.089} = 0.5 \mu\text{g}\cdot\text{L}^{-1}$$

Therefore, a difference in concentration of $0.5 \mu\text{g}\cdot\text{L}^{-1}$ between two different solutions of mercury increases the absorbance by 1%.

Limit of detection

For the determination of the limit of detection the standard deviation of the constant b (s_b) was obtained and applied to equation 5 as follow:

$$LOD = \frac{3.3 \times s_b}{m} = \frac{3.3 \times 0.0009 \mu\text{g. L}^{-1}}{0.0083} = 0.3 \mu\text{g. L}^{-1}$$

This value indicates that with 95% of confidence it's possible to detect mercury in concentrations equal to or higher than $0.3 \mu\text{g. L}^{-1}$ in soil extracts using this methodology.

Limit of quantification

Similar to the determination of the limit of detection, the limit of quantification was obtained using s_b and equation 6.

$$LOQ = \frac{10 \times s_b}{m} = \frac{10 \times 0.0009 \mu\text{g. L}^{-1}}{0.0083} = 1.0 \mu\text{g. L}^{-1}$$

Thus, the adopted methodology is capable of quantifying with a good precision mercury in concentrations equal to or higher than $1.0 \mu\text{g. L}^{-1}$ in soil extracts with 95% of confidence.

3.3. Case of study: Fojo waste pile of Pejão mining complex

3.3.1. *Aqua regia* extractable content of Hg in soil samples

As stated before, a variety of acids and mixtures can be used for microwave digestion of soil samples. However, in this work, due to the hazardous potential of other acid mixtures a microwave assisted digestion procedure using *aqua regia* was adopted.

This method is less aggressive than procedures that use mixtures of stronger acids, such as HF and HClO₄, and the obtained extracts are commonly considered to represent “pseudo-total” concentrations of the analyte in the sample. Nonetheless, recent studies reported that digestion procedures with *aqua regia* can yield, for several metals, statistically similar performance to procedures using more aggressive acid mixtures.^[25,29]

In this work, the *aqua regia* soluble (or pseudo-total content) Hg in soil samples was first determined to assess the contamination of the mine region by this element considering the worst possible scenario, that all the mercury in soil would be bioavailable

for contamination of surrounding soils, aquifers and ecosystems. After the soil samples digestion, the Hg contents in extracts was determined by CV-AAS.

Soil samples were collected from four zones of the Fojo mine region: (a) waste pile affected by combustion (“escombreira ardida”, EA), (b) waste pile non-affected by combustion (“escombreira não-ardida”, ENA), (c) downstream soil region (“solo a jusante”, SJ) and (d) upstream soil region (“bosque”, B). The latter zone was intentionally sampled to be used as regional background assuming that it is not contaminated by Hg due to the fact of being located in an upstream region relatively to the waste pile.

Table 88 compiles the pseudo-total concentration of Hg in all samples collected from the deactivated Pejão coal mining complex. For clarity, data obtained is also graphically represented in **Figure 17**.

The obtained values for Hg in soil samples, ranging from 0.1 to 1.2 mg.kg⁻¹, are above the background values for Portugal reported in project FOREGS (between 0.017 and 0.080 mg.kg⁻¹)^[50] showing an enrichment of Hg in the mine region from anthropogenic sources.

Table 8 - Hg aqua regia soluble content in Pejão coal mine samples (EA, ENA, B and SJ).

Hg pseudo-total concentration							
Sample	Hg (mg.kg ⁻¹) (± 0.1 mg.kg ⁻¹) ^(a)	Sample	Hg (mg.kg ⁻¹) (± 0.1 mg.kg ⁻¹) ^(a)	Sample	Hg (mg.kg ⁻¹) (± 0.1 mg.kg ⁻¹) ^(a)	Sample	Hg (mg.kg ⁻¹) (± 0.1 mg.kg ⁻¹) ^(a)
EA1	1.2	ENA1	0.9	B1	0.1(0.08) ^(b)	SJ1	0.1
EA2	0.7	ENA2	0.5	B2	0.1(0) ^(b)	SJ2	0.5
EA3	1.0	ENA3	0.8	B3	0.1(4) ^(b)	SJ3	0.2
EA4	0.8	ENA4	1.0	B4	0.1(2) ^(b)	SJ4	0.5
EA5	0.8	ENA5	0.7	B5	0.1(2) ^(b)	SJ5	0.2
EA6	0.8	Min	0.5	Min	0.1(0.08) ^(b)	Min	0.1
EA7	1.1	Max	1.0	Max	0.1(4) ^(b)	Max	0.5
EA8	0.9	Mean	0.8	Mean	0.11	Mean	0.3
EA9	0.9	SD	0.2	SD	0.02	SD	0.2
EA10	1.0						
Min	0.7						
Max	1.2						
Mean	0.9						
SD	0.2						

^(a) precision calculated with equation:
$$s = \sqrt{\frac{(y_1 - y'_1)^2}{2} + \frac{(y_2 - y'_2)^2}{2} + \dots + \frac{(y_n - y'_n)^2}{2}}{n}$$

^(b) Value considered to better visualize the variation shown in the graphic bellow

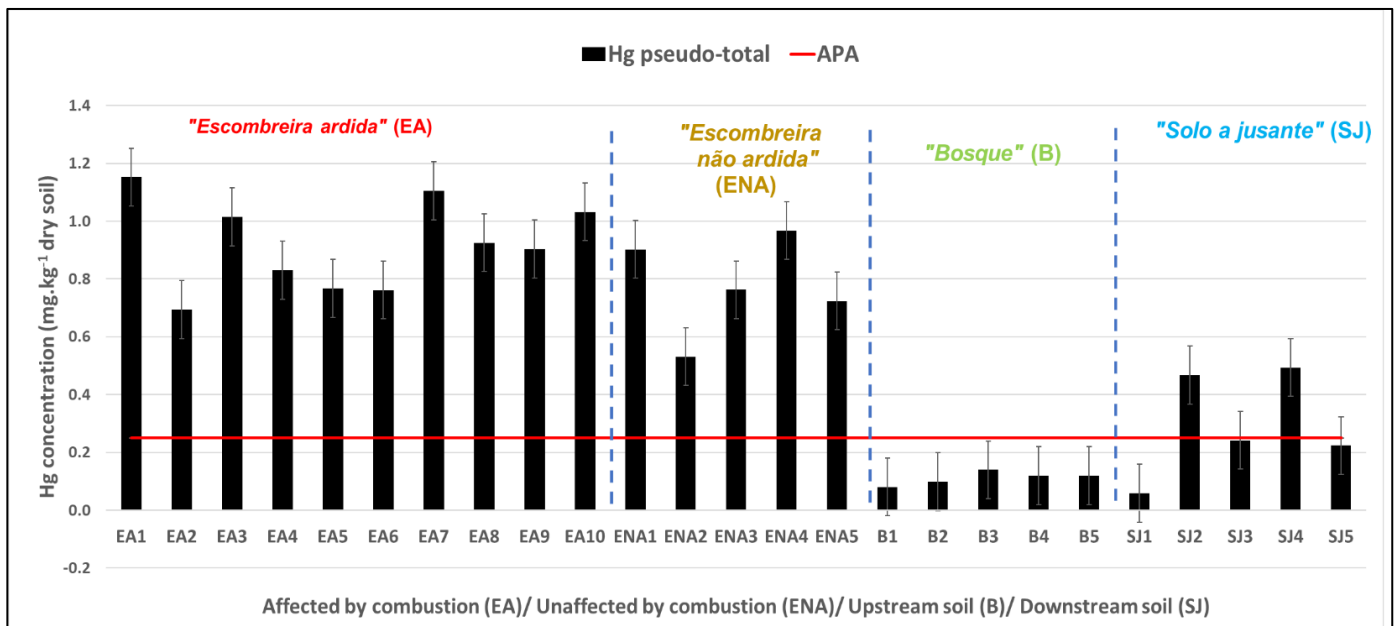


Figure 17 - Graphical representation of the obtained aqua regia soluble content of Hg in Pejão coal mine samples (EA, ENA, B and SJ). APA reference value represented by the red line.

The *Agência Portuguesa do Ambiente* (APA) technical guide for contaminated soils^[51] available for viewing on their website mentions the reference values for a given contaminant according to the location of the sample relatively to specific regions, such as environmentally sensitive sites and water bodies, and characteristics of the soil (texture and soil depthness). Following the guide's chart, the proper reference value for the Fojo mine region was found in Table C of APA's guide. For a more restrictive approach, the value for agricultural use soils was used (0.25 mg.kg^{-1} ; red line in **Figure 17**) since agriculture is a common practice in the surrounding region.

As can be seen, all samples from EA and ENA zones showed concentration values for mercury higher than APA's reference value (0.25 mg.kg^{-1}). Furthermore, mean values of the samples from regions EA (0.9 mg.kg^{-1}) and ENA (0.8 mg.kg^{-1}) are respectively about 800% and 700% higher than the mean value of the selected reference region (samples B1-5; 0.11 mg.kg^{-1}), revealing a very concerning accumulation of this PTE in the region and indicating that the waste pile zones are the main source of anthropogenic Hg contamination in this region.

Samples from the downstream region (SJ) presented values close to APA's reference value and a mean value (0.3 mg.kg^{-1}) about 200% higher than the mean value of the reference samples (B; 0.11 mg.kg^{-1}). This increase is likely related to the spread

of the contamination due to erosion and/or lixiviation from the waste pile to the surrounding soils and groundwater.

Finally, as expected, each sample from zone B, the background region, showed an average concentration of mercury below the APA reference value.

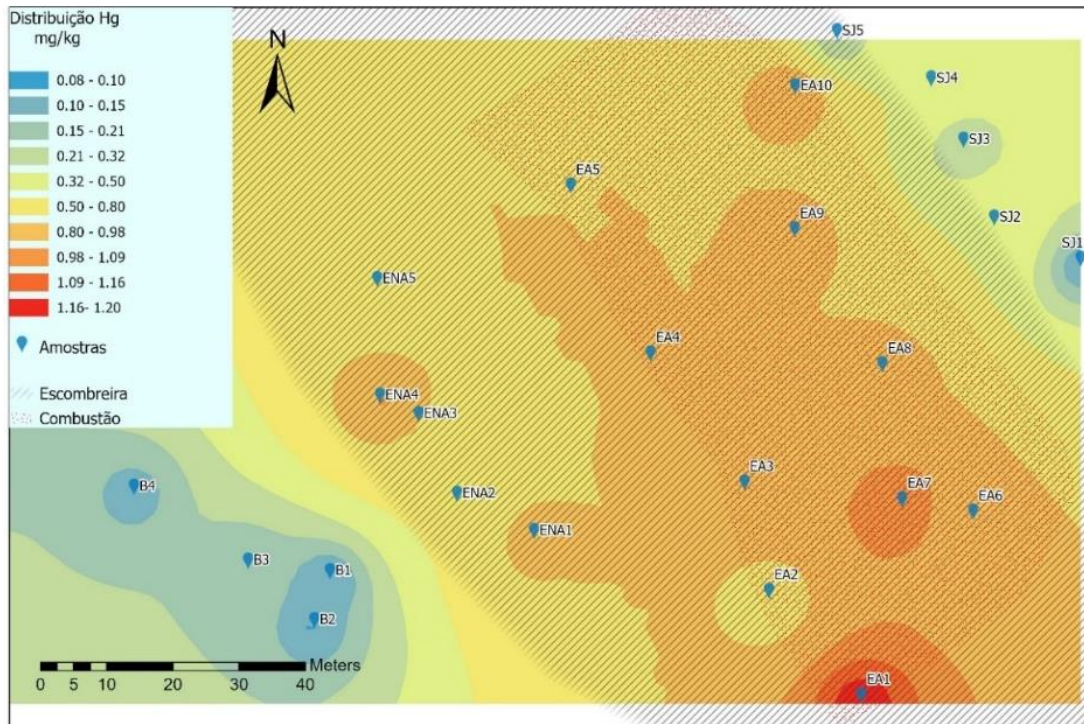


Figure 18 - Map of colors of Hg distribution in Fojo waste pile and surrounding region.

For a better observation of the spatial distribution of Hg in the Fojo mine area, an inverse distance weighted (IDW) interpolation map was built and provided by the GAOT department of the university of Porto using the Geostatistical tool of the ArcGIS Pro software utilizing Hg pseudo total values, as shown in **Figure 18**. As can be seen in this map, the Hg concentration increases when going from colder colors (blue) to hotter colors (red). The blue region contains the soil samples selected as background (B) that are located at an upstream region relatively to the waste piles. The orange area, where the contamination is centered and from where it spreads, is mainly composed of samples from the waste pile affected by the fires (EA). Finally, the yellow region contains the waste pile samples not affected by the fires (ENA) and the samples from the downstream region (SJ) relatively to the waste piles.

The geoaccumulation index (I_{geo}) is commonly used to classify and determine the level of contamination of soils by heavy metals.^[52,53] It considers the national background

average concentration of the PTE and accounts for possible variations due to the natural heterogeneity of the soils.^[52]

The geoaccumulation index is calculated based on the equation:

$$I_{geo} = \log_2(C_i/1.5B)$$

where C_i is the measured concentration of the metal in $mg.kg^{-1}$, B is the corresponding national background average concentration and the factor 1.5 considers the soil heterogeneity.

Based on the I_{geo} value, samples are classified in the different classes, as shown in **Table 99**.

Table 9 - Geoaccumulation index classification chart.

Class	I_{geo}	Definition
0	$I_{geo} < 0$	Unpolluted
1	$0 < I_{geo} < 1$	Unpolluted to moderately polluted
2	$1 < I_{geo} < 2$	Moderately polluted
3	$2 < I_{geo} < 3$	Moderately to strongly polluted
4	$3 < I_{geo} < 4$	Strongly polluted
5	$4 < I_{geo} < 5$	Strongly to extremely polluted
6	$5 < I_{geo}$	Extremely polluted

The obtained I_{geo} values, using project FOREGS reported mean value for Portugal, for each sample are summarized in **Table 1010**. Briefly, and based on the estimated I_{geo} values, the samples from the wastes piles (EA and ENA) were classified as “strongly polluted” and the samples from the downstream region (SJ) were considered to be “moderately to strongly polluted”. These classifications further highlight that the waste piles are a concerning source of contamination to this area. As expected, samples from the upstream region (B) fall in the category “unpolluted to moderately polluted”.

Table 10 - Calculated geoaccumulation index for all Pejão coal mine samples (EA, ENA, B and SJ).

Geoaccumulation index (I_{geo})							
Sample	I_{geo}	Sample	I_{geo}	Sample	I_{geo}	Sample	I_{geo}
EA1	4.0	ENA1	3.6	B1	0.14	SJ1	-0.3
EA2	3.3	ENA2	2.9	B2	0.44	SJ2	2.7
EA3	3.8	ENA3	3.4	B3	0.94	SJ3	1.7
EA4	3.5	ENA4	3.7	B4	0.71	SJ4	2.8
EA5	3.4	ENA5	3.3	B5	0.72	SJ5	1.6
EA6	3.4						
EA7	3.9						
EA8	3.7						
EA9	3.6						
EA10	3.8						

Considering that the obtained Hg pseudo-total concentration values in the mine region were mostly higher than APA's reported reference value, a sequential extraction procedure (SEP) was applied to fractionate the Hg species and better assess its mobility and risk to the environment.

3.3.2. Mercury fractionating

The procedure described in USEPA 3200^[22] was chosen in this work to fractionate mercury species into mobile, semi-mobile and non-mobile fractions. Briefly, the mobile fraction contains mainly organic and inorganic Hg²⁺ species bioavailable for soil-to-plant transfer^[4]. The semi-mobile fraction mostly contains elemental Hg and possibly amalgams and the non-mobile fraction is mainly composed by sulfides and calomels of mercury.

After application of the three-step extraction procedure to the same soil sample, the obtained Hg values in sample extracts are summarized in **Table 11**. Furthermore, the results displayed in the table are graphically represented in **Figure 19**. The data obtained allowed to conclude that, for all samples, the most dominant fraction is the semi-mobile fraction with an average mercury concentration value of 0.5 mg.kg⁻¹, ranging from 0.05 mg.kg⁻¹ to 1.04 mg.kg⁻¹. Furthermore, the Hg content in the semi-mobile fraction is higher than APA's reference value for agricultural use soils (0.25 mg.kg⁻¹; red line in **Figure 19**), except for the background region (B). The obtained levels of mercury in the semi-mobile fraction are concerning and can pose a risk to the environment as even

though this fraction mainly contains species of mercury that are not readily bioavailable, they can be easily converted into more labile species.^[4,12]

Table 11 - Hg concentration (mg.kg⁻¹) in each extracted fraction for Pejão coal mine samples (EA, ENA, B and SJ).

Sample	Mobile Hg (mg.kg ⁻¹) (± 0.02 mg.kg ⁻¹)	Semi-mobile Hg (mg.kg ⁻¹) (± 0.09 mg.kg ⁻¹)	Non-mobile Hg (mg.kg ⁻¹) (± 0.01 mg.kg ⁻¹)
EA1	0.16	0.74	0.09
EA2	0.10	0.58	0.08
EA3	0.16	0.76	0.09
EA4	0.16	0.70	0.07
EA5	0.12	0.43	0.07
EA6	0.11	0.58	0.09
EA7	0.22	1.04	0.09
EA8	0.13	0.57	0.06
EA9	0.15	0.90	0.11
EA10	0.16	0.68	0.09
Min	0.10	0.43	0.06
Max	0.22	1.04	0.11
Mean	0.15	0.7	0.08
SD	0.03	0.2	0.01
ENA1	0.05	0.27	0.08
ENA2	0.03	0.27	0.09
ENA3	0.04	0.56	0.11
ENA4	0.09	0.79	0.10
ENA5	0.04	0.53	0.17
Min	0.03	0.27	0.08
Max	0.09	0.79	0.17
Mean	0.05	0.5	0.11
SD	0.02	0.2	0.03
B1	< LOQ	0.05	< LOQ
B2	< LOQ	0.06	< LOQ
B3	< LOQ	0.14	< LOQ
B4	< LOQ	0.11	< LOQ
B5	< LOQ	0.07	< LOQ
Min	-	0.05	-
Max	-	0.14	-
Mean	-	0.09	-
SD	-	0.04	-
SJ1	< LOQ	< LOQ	< LOQ
SJ2	0.06	0.40	0.13
SJ3	0.07	0.32	0.07
SJ4	0.07	0.37	0.03
SJ5	0.06	0.29	< LOQ
Min	0.06	0.29	0.03
Max	0.07	0.40	0.13
Mean	0.07	0.35	0.08
SD	0.01	0.05	0.05

(a) precision for each extracted fraction was calculated with equation: $s = \sqrt{\frac{(y_1 - y'_1)^2}{2} + \frac{(y_2 - y'_2)^2}{2} + \dots + \frac{(y_n - y'_n)^2}{2}}$

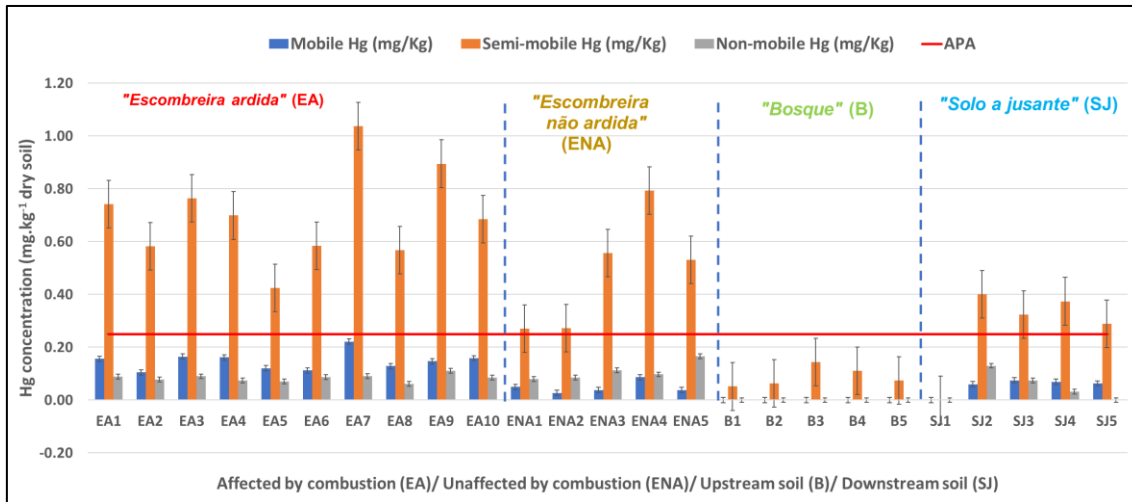


Figure 19 – Graphical representation of Hg concentration (mg.kg⁻¹) in each extracted fraction for Pejão coal mine samples (EA, ENA, B and SJ).

In the main source of contamination, the waste piles affected and unaffected by combustion, the distribution of Hg through the mobile and non-mobile fractions is interestingly different. For samples from the waste pile region affected by combustion (EA), the second most dominant fraction is the mobile fraction with an average value of 0.15 mg.kg⁻¹ (16% of the sum of fractions) and with values ranging from 0.10 mg.kg⁻¹ to 0.22 mg.kg⁻¹. In contrast, for samples from the unaffected waste pile (ENA), the second most dominant fraction is the non-mobile fraction (17% of the sum of fractions), with Hg concentration ranging from 0.08 mg.kg⁻¹ to 0.17 mg.kg⁻¹ and an average concentration value of 0.11 mg.kg⁻¹.

At this point, it was of interest to understand the influence of the combustion in the distribution of mercury through the different fractions between the waste piles unaffected and affected by the fire. For that, the obtained concentration values for the mobile fraction in both regions (EA and ENA) were further statistically compared. The statistical analysis, consisting of F-test using ANOVA, allowed to conclude that Hg levels in the mobile fraction between the two waste pile areas were significantly different despite of the heterogeneous nature of the samples. This strongly suggests that the combustion of the waste pile (EA) affected the mobility and distribution of Hg, being the most probable reason for the increase of the mercury content in the mobile fraction relatively to EA samples, similarly to the observed in other studies of coal waste piles affected by combustion where it was reported that the fire was responsible for the increase in the concentration of several PTEs in the soil.^[9]

According to the literature^[54], Hg can be found in coal bound to the organic matrix, sorbed as elemental Hg, in isomorphous sulfides structures and bound to silica minerals. The release of Hg through thermal decomposition varies according to the Hg species and the way they are bound. For example, adsorbed Hg is released at temperatures below 200 °C and pyrite bound Hg starts to be released at temperatures ranging from 350 °C to 600 °C, when the lattice destruction occurs.

In the soil downstream to the waste piles (SJ), the second most dominant fraction was the mobile fraction, with Hg levels ranging from 0.03 mg.kg⁻¹ to 0.07 mg.kg⁻¹ and with an average value of 0.05 mg.kg⁻¹. This increase in Hg concentration relatively to the lower concentrations found in samples from the upstream soil region (B, background) can possibly be explained by the spread of contamination through the years from the waste piles (particularly the one affected by combustion, EA) by lixiviation and/or erosion.

From the obtained data it is clear the negative environmental impact of coal mining in this region. Considering that the nearby soils of this region are used for agriculture and livestock, the risk posed by the high amount of mercury in the mobile (near the APA reference value for some samples) and semi-mobile fractions (higher than APA reference value) underlines the need for control, monitoring and possible intervention in the region. The impact of forest fires in the increase in mercury release to the soil also alerts for the need of taking measures for the proper disposal and/or treatment of mine waste materials as it emphasizes the environmental risks arising from unprotected and exposed mine wastes.

3.4. Case of study: Poça da cadela wolframium mine in Regoufe

3.4.1. *Aqua regia* extractable content of Hg in soil samples

Sampling sites in the Regoufe mine were not divided in different zones as the previous case of study. Besides, no background samples were collected. In this region, the samples were collected close to the mine entrances, along the ore processing line and the mine drainage line, and at the waste piles (of both thin and bulk materials).

The pseudo-total concentrations of Hg were also obtained by microwaved assisted digestion for all the samples collected in the Regoufe mine. The obtained values are summarized at the **Table 122** and also represented in **Figure 20**.

Table 12 - Hg *aqua regia* soluble content for Regoufe mine samples

Sample	Hg (mg.kg ⁻¹) (± 0.8 mg.kg ⁻¹) ^(a)
R1	2.6
R2	6.8
R4	3.4
R5	6.9
R6	2.1
R7	2.7
R8	3.3
R9	2.2
R12	1.6
R13	0.4
R14	5.3
R15	1.3
R16	2.8
R17	3.0
R18	0.9
R21	0.6
R22	0.4
R23	0.6
R25	0.4
R27	0.6
Min	0.4
Max	6.9
Mean	2
SD	2

^(a) precision calculated with equation:
$$s = \sqrt{\frac{\frac{(y_1 - y'_1)^2}{2} + \frac{(y_2 - y'_2)^2}{2} + \dots + \frac{(y_n - y'_n)^2}{2}}{n}}$$

As can be seen, the results obtained for this mine region showed a high variability in the pseudo-total concentration of mercury between the different samples. The obtained Hg concentration values for the Regoufe mine ranged from 0.4 mg.kg⁻¹ to 6.9 mg.kg⁻¹ with an average value of 2 mg.kg⁻¹. These values are highly above the reported background values for Portugal in project FOREGS (between 0.017 and 0.080 mg.kg⁻¹), showing an enrichment of mercury relatively to national background values. This enrichment can be due to anthropogenic activity or due to the natural diversity of mineral that compose the soil.

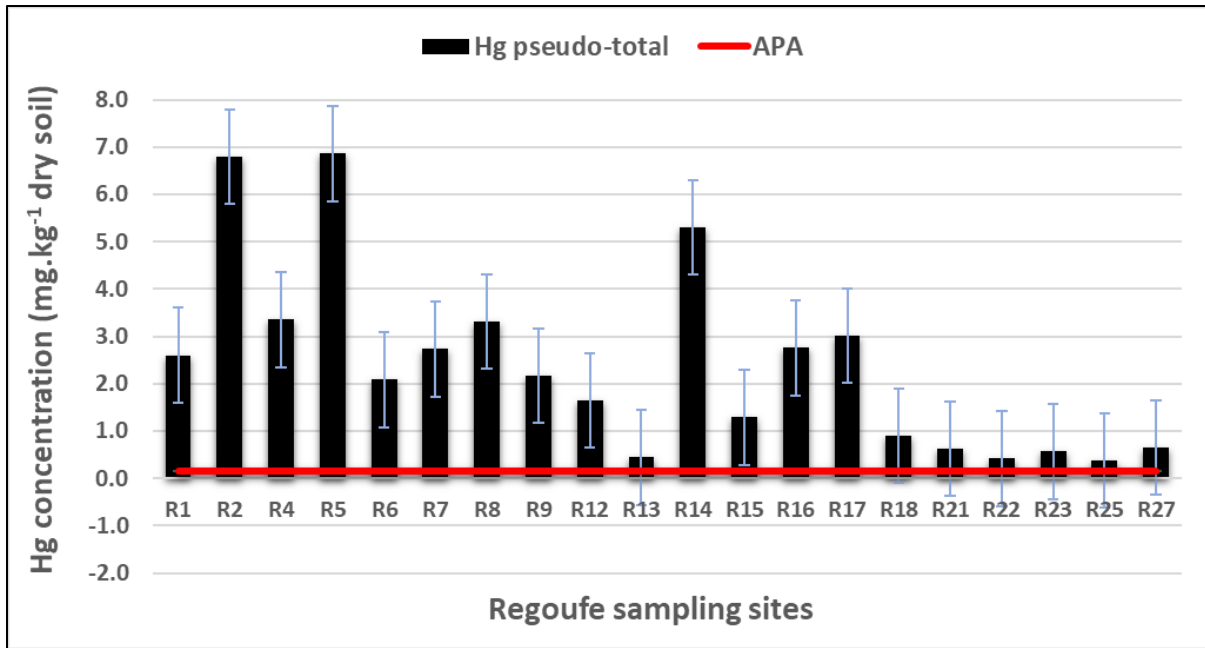


Figure 20 - Graphical representation of the obtained *aqua regia* soluble content of Hg in Pejão coal mine samples. APA reference value represented by the red line.

Comparing the two mines under study, the average levels of Hg found in the soil extracts for the Regoufe mine (2 mg.kg⁻¹) is about four times higher than the average value obtained for the Fojo waste pile region (0.6 mg.kg⁻¹). These results are in agreement with a recent study that reported lower concentrations of other PTEs in soils from coal mines relatively to metal mines.^[55]

From IDW map created using the collected data, represented in **Figure 21**, we can easily observe that samples R2, R5 and R14 have higher Hg concentration in comparison to other samples collected very nearby. Sample R2 is located at the waste pile of thin residues, sample R5 is located in a downstream region relatively to where the mineral processing occurred and sample R14 is located near the entrance of one of the mines shafts. Thus, from the results obtained, it is not possible to provide any reason why the Hg concentration in these points is considerably higher relatively to the other sampling sites. Besides, according to historical information about this mine, mercury was not involved in the ore processing techniques used to refine the minerals, making anthropogenic contamination less probable. In this manner, the results suggests that the variability of Hg levels observed may be related to the high heterogeneity of the collected soil samples in terms of Hg distribution.

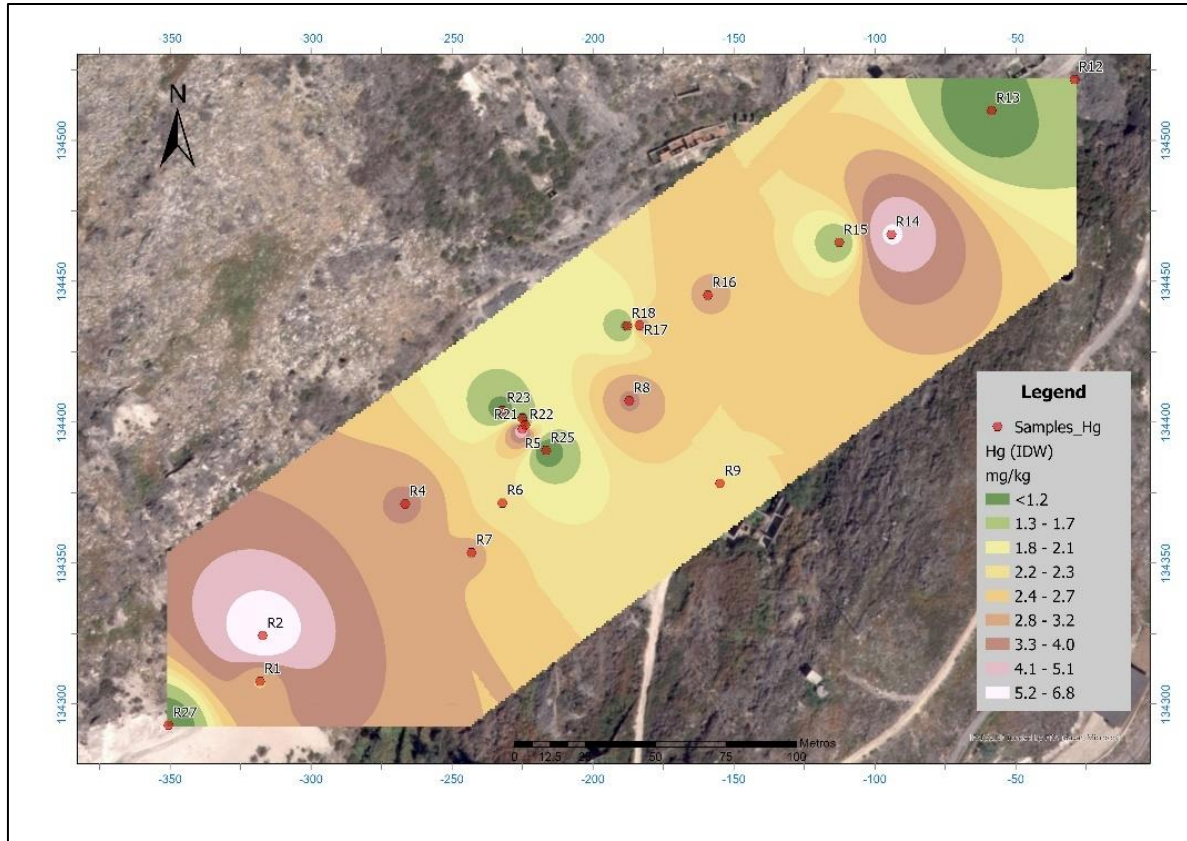


Figure 21 - Map of colors of Hg distribution in Fojo waste pile and surrounding region.

The I_{geo} values were also calculated for all of the collected samples in Regoufe mine and are summarized in **Table 133**. In general, 45% of the samples were considered “extremely polluted”, 20% “strongly to extremely polluted”, 15% “strongly polluted” and 20% “moderately to strongly polluted”.

Relatively to the APA’s reference value, this mine region is included in the Natura2000 network under the habitat’s directive sites and therefore the reference value for agricultural use soil is lower than for Fojo mine (of 0.16 mg.kg^{-1} , found in Table A of APA’s guide). As can be easily seen in **Figure 20**, all analyzed soils samples have Hg levels above the reported reference value (represented by the red line in the graphic).

Table 13 - Calculated geoaccumulation index for all Regoufe mine samples.

Geoaccumulation index	
Sample	I _{geo}
R1	2.4
R2	2.5
R4	2.6
R5	3.0
R6	3.1
R7	3.2
R8	3.6
R9	4.1
R12	4.5
R13	4.8
R14	4.9
R15	5.2
R16	5.2
R17	5.2
R18	5.4
R21	5.5
R22	5.5
R23	6.2
R25	6.5
R27	6.6

Taking into consideration the high contents of mercury in Regoufe soil samples relatively to the APA's reference value and the information provided by the geoaccumulation index, the SEP was applied to assess mercury's relative mobility and bioavailability and to evaluate its potential environmental impact in the mine surrounding ecosystems.

3.4.2. Mercury fractioning

The USEPA3200 procedure was also applied in this work to the Regoufe mine samples. The concentrations of Hg in each fraction for the collected samples are summarized in **Table 144** and also represented in **Figure 22**.

Table 14 - Hg concentration (mg.kg⁻¹) in each extracted fraction for Regoufe mine samples.

Sample	Mobile Hg (mg.kg ⁻¹)	Semi-mobile Hg (mg.kg ⁻¹)	Non-mobile Hg (mg.kg ⁻¹)
	(± 0.01 mg.kg ⁻¹) ^(a)	(± 0.05 mg.kg ⁻¹) ^(a)	(± 0.07 mg.kg ⁻¹) ^(a)
R1	0.11	0.12	0.04
R2	0.48	0.16	0.05
R4	0.46	0.17	0.14
R5	0.12	0.36	0.36
R6	0.11	0.44	0.22
R7	0.19	0.48	0.10
R8	0.07	0.36	0.23
R9	< LOQ	0.22	0.12
R12	0.04	0.18	< LOQ
R13	0.02	0.26	0.03
R14	0.19	0.19	0.21
R15	0.04	0.23	0.09
R16	0.10	0.32	0.34
R17	< LOQ	0.24	0.22
R18	< LOQ	0.12	0.11
R21	< LOQ	0.28	0.34
R22	< LOQ	0.27	0.25
R23	< LOQ	0.25	0.17
R25	< LOQ	0.29	0.24
R27	< LOQ	0.34	0.14
Min	0.02	0.12	0.03
Máx	0.48	0.48	0.36
Mean	0.16	0.26	0.18
SD	0.1	0.1	0.1

^(a) precision for each extracted fraction was calculated with equation:
$$s = \sqrt{\frac{\frac{(y_1 - y'_1)^2}{2} + \frac{(y_2 - y'_2)^2}{2} + \dots + \frac{(y_n - y'_n)^2}{2}}{n}}$$

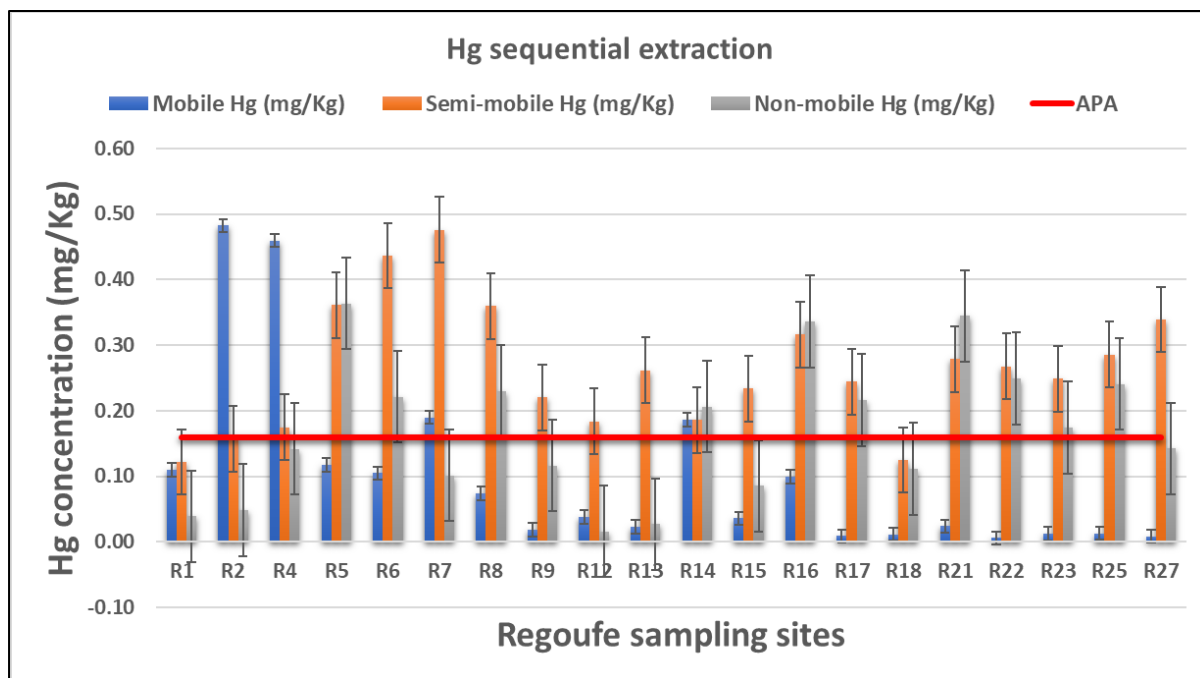


Figure 22 - Graphical representation of Hg concentration (mg.kg^{-1}) in each extracted fraction for Regoufe mine samples

The SEP revealed a difference in mercury mobility between the two studied regions. It's easy to understand that higher organic matter content is found in the coal mine soil rather than the mine soil, and since organic matter content in soil plays a significant role in the retention of heavy metals this is the most probable reason for the higher percentage of mercury in the non-mobile fraction.^[4,12,23,56]

It was also observed that the semi-mobile fraction is the most dominant fraction for most of the Regoufe mine samples corresponding to 49% of the average total extracted mercury. An average value of 0.26 mg.kg^{-1} (with values ranging from 0.12 mg.kg^{-1} to 0.48 mg.kg^{-1}) was estimated, revealing that for almost all samples, the semi-mobile fraction concentrations of Hg are above the APA's reference value for agricultural use (0.16 mg.kg^{-1}).

The mobile fraction showed a high variability in Hg levels from sample to sample, with concentrations ranging from 0.01 mg.kg^{-1} to 0.48 mg.kg^{-1} and an average of 0.10 mg.kg^{-1} . The Hg concentration is particularly concerning in some samples, namely samples R2, R4, R7 and R14, where the values are above APA's reference value. R4 and R7 sampling sites are at a downstream region relatively to R2 sampling site, and therefore the higher content of Hg in the mobile fraction for those samples may be an indication of the direction which the contamination spreads from sample R2.

As can be observed in **Figure 22**, the non-mobile fraction shows no discerning pattern. The concentration of Hg in this fraction ranges from 0.02 mg.kg⁻¹ to 0.36 mg.kg⁻¹ with an average of 0.17 mg.kg⁻¹.

However, before any final conclusion regarding the environmental impact of Hg in this region, it's important to consider that the SEP methodology appears to have critical limitations when applied to this case of study. For this mine region the recovery values were rather low, ranging from 10 to 30%. This means that the sum of Hg content in the three fractions of SEP (mobile, semi-mobile and non-mobile) represented a low percentage of the pseudo-total Hg (*aqua regia* extractable content of mercury) for most of the samples. For comparison, recovery values from 70 to 120% were obtained for the samples of the Fojo waste pile of the Pejão coal mine.

Two possible explanations for this phenomenon are:

(1) the Hg in this mine region is mostly found associated to soil matrix and, therefore, being part of soil crystalline composition or;

(2) the SEP method chosen in this work is not the most suitable for this kind of mine soil which contains higher levels of Hg than coal mines, for example.

In order to fully understand the results obtained the repetition of the SEP procedure is strongly recommended to achieve reliable results. In addition, the remaining soil samples collected should be further subjected to a microwave assisted digestion with *aqua regia* to extract the residual content of mercury. If high concentrations of Hg were found, then the first hypothesis would be proven true, meaning that Hg is strongly bound to the soil matrix components and even after the three-steps of extraction Hg can't be fully extracted.

Finally, the SEP method should be further studied, and if the second hypothesis is proven to be true the suitability of other SEP methods, such as modified BCR or CIEMAT procedures^[16], to the soil characteristics should be tested.

4. Conclusions and future work

Active and deactivated mining sites are nowadays one of the major anthropogenic sources of heavy metal to the environment. The wastes from mine activity usually contain a high content of heavy metals and, when exposed to air and water, can undergo oxidation and produce sulfuric acid that can easily mobilize the heavy metals to the surrounding soil and groundwater, and ultimately disrupt the environment and affect living beings.

In this work, the Fojo waste pile region of the deactivated Pejão coal mine complex, located at Castelo de Paiva municipality, and the deactivated W-Sb mine Poça da Cadela, located in Regoufe, were studied to assess their potential environmental impact in surrounding soils and aquifers. This study focused on the determination of mercury content in soil since it is a critical soil contaminant of high toxicity to plants and organisms and which few data on its speciation can be found in the literature.

First, the total amount of mercury in mine soil samples was estimated. The determination of the *aqua regia* soluble content of Hg was successfully performed using a microwave assisted digestion method, based on ISO 12914 and USEPA 3051A, to assess the scale of soil contamination with Hg.

This approach was chosen in this work due to being faster, safer, less time-consuming and requires less amount of sample and reagents than other conventional methods and its using acid mixtures with HF and HClO₄. Furthermore, in future work, the method will be validated for Hg by using a reference soil material.

As stated before, PTEs bioavailability and toxicity to organisms is strongly influenced by the chemical forms in which they are found in the environment (speciation). Therefore, the analysis of the total PTEs content in the soil is not enough to assess the environment risks to human health and ecosystems. Thus, in this work, the three-step sequential extraction procedure USEPA 3200 was applied to fractionate Hg into the mobile, semi-mobile and non-mobile fractions in order to evaluate Hg bioavailability to the mines surrounding soils and groundwater's.

The quantification of Hg in mine soil samples was performed by CV-AAS technique. Thus, in the first part of this work, optimization of some chemical and operational variables was performed to improve detection sensitivity while minimizing sample consumption. Based on literature consulted, solutions of 1% (w/v) NaBH₄ (stabilized in 0.5% (w/v) NaOH) and 10% (v/v) HCl were adopted as reagents for the

generation of Hg cold vapor. Moreover, a pump speed of 40 rpm and an inert gas (N_2) flow rate of $100 \text{ mL}\cdot\text{min}^{-1}$ were chosen for analysis. Nonetheless, this optimization also intended to consider the possibility of using the same conditions for the analysis of other heavy metals, such as arsenic (As) and antimony (Sb), by hydride generation (HG-AAS).

Due to the small volume of sample available it was also necessary to minimize the sample consumption. Therefore, the analysis procedure consisting of 100 s analysis was modified to an initial resting time of 10 s, followed of a sample aspiration time of only 25 s (instead of 100s), and a final resting time of 65 s. This modification allowed to for the minimization of the sample consumption (approximately 4 mL per analysis) without compromising the analytical limits. With this approach a LOD of $0.3 \mu\text{g}\cdot\text{L}^{-1}$ and a LOQ of $1.0 \mu\text{g}\cdot\text{L}^{-1}$ were obtained with 95% of confidence, allowing for trace analysis of Hg in soil samples.

In this work, the results obtained demonstrated an enrichment of Hg in Fojo coal waste pile region relatively to regional ("Bosque" samples) and national background values (FOREGS value), with concentration levels exceeding APA's reference value for agricultural use soils at the wastes piles (zones EA, ENA) and at the downstream region (SJ). Furthermore, the waste piles both, affected (EA) and non-affected (ENA) by combustion, showed to be the major source of Hg contamination to the surrounding soils and groundwater's, being classified according to estimated geoaccumulation index values as "strongly polluted" areas.

After application of the SEP method to this mine region, it was possible to conclude that the most dominant fraction was the semi-mobile fraction. Nonetheless, significant amounts of Hg were also found in the mobile fraction for some samples, particularly for the waste pile affected by the fires (EA). The results obtained suggest that the combustion of the waste pile affected the mercury bioavailability due to releasing of Hg from the pile materials through thermal decomposition which explains the higher percentage of Hg found in the mobile fraction in the waste pile affected by combustion (EA) relatively to the non-affected waste pile (ENA). In addition, the downstream soil relatively to the waste pile (SJ) showed an increase in mercury content when compared to the upstream soil (B) probably as a result of the spread of the contamination through erosion and lixiviation.

in this case of study, the obtained data for Hg revealed the negative environmental impact in the region caused by coal mining and the need for control and monitoring of heavy metals and possible intervention in this mine region. This study also emphasizes the environmental risk arising from unprotected and exposed mine wastes.

Relatively to the Regoufe mine, the pseudo-total Hg results showed an enrichment of this PTE in the mine soil samples when compared to Portugal background values, and a general increase of Hg content relatively to the Fojo coal waste pile region. Furthermore, the content of Hg in all samples exceeded APA's reference value and the geoaccumulation index values determined classified this mine region as "moderated to extremely" contaminated.

The SEP applied in this case of study revealed that the semi-mobile fraction was also the most dominant fraction. However, for few samples, the concentration of Hg in the mobile fraction exceeds the APA's reference value, pointing to a threatening Hg contamination of the area that can be further increased by the conversion of the semi-mobile species into more mobile species.

Nonetheless, despite the USEPA 3200 SEP method being considered a reference method for Hg fractioning in soils, the methodology showed some critical limitations for the Regoufe mine since recovery was very low. Thus, further assays should be performed to confirm and understand the SEP results obtained for Hg in the Regoufe mine. In this context, the remaining soil samples should be further submitted to a final *aqua regia* digestion to estimate the residual Hg content. This will allow to verify the possibility of the Hg being strongly bound to the soil matrix, being part of the crystalline structure of some rocks and minerals, thus requiring more aggressive methods to extract Hg. Otherwise, a different SEP method should be applied to this mine region.

In future work, other SEP methods may also be applied to study other PTEs, namely:

- (i) As and Sb, since preliminary assays (see annex I) revealed that Fojo waste pile region shows an enrichment of those metalloids relatively to reported background values for Portugal in project FOREGS. The SEP method reported by Shiowatana *et. al.*, described in **Annex II**, will be applied for these two elements after preliminary bibliographic research performed.
- (ii) Cd, Pb, Cr, Zn, Cu and Ni, using the three-step modified BCR procedure and performing the analysis of the extracts using eletrothermal atomic absorption spectroscopy (ET-AAS). Preliminary tests regarding optimization and establishment of concentration ranges were already performed.

5. Bibliography

- (1) Jaishankar, M.; Tseten, T.; Anbalagan, N.; Mathew, B. B.; Beeregowda, K. N. Toxicity, Mechanism and Health Effects of Some Heavy Metals. *Interdiscip. Toxicol.* **2014**, *7* (2), 60–72. <https://doi.org/10.2478/intox-2014-0009>.
- (2) Musilova, J.; Arvay, J.; Vollmannova, A.; Toth, T.; Tomas, J. Environmental Contamination by Heavy Metals in Region with Previous Mining Activity. *Bull. Environ. Contam. Toxicol.* **2016**, *97* (4), 569–575. <https://doi.org/10.1007/s00128-016-1907-3>.
- (3) Demková, L.; Jezný, T.; Bobulská, L. Assessment of Soil Heavy Metal Pollution in a Former Mining Area-before and after the End of Mining Activities. *Soil Water Res.* **2017**, *12* (4), 229–236. <https://doi.org/10.17221/107/2016-SWR>.
- (4) Reis, A. T.; Davidson, C. M.; Vale, C.; Pereira, E. Overview and Challenges of Mercury Fractionation and Speciation in Soils. *TrAC - Trends Anal. Chem.* **2016**, *82*, 109–117. <https://doi.org/10.1016/j.trac.2016.05.008>.
- (5) Karn, R.; Ojha, N.; Abbas, S.; Bhugra, S. A Review on Heavy Metal Contamination at Mining Sites and Remedial Techniques. *IOP Conf. Ser. Earth Environ. Sci.* **2021**, *796* (1). <https://doi.org/10.1088/1755-1315/796/1/012013>.
- (6) Cohen, R. R. H. Use of Microbes for Cost Reduction of Metal Removal from Metals and Mining Industry Waste Streams. *J. Clean. Prod.* **2006**, *14* (12-13 SPEC. ISS.), 1146–1157. <https://doi.org/10.1016/j.jclepro.2004.10.009>.
- (7) Alvarenga, P.; Guerreiro, N.; Simões, I.; Imaginário, M. J.; Palma, P. Assessment of the Environmental Impact of Acid Mine Drainage on Surface Water, Stream Sediments, and Macrophytes Using a Battery of Chemical and Ecotoxicological Indicators. *Water* **2021**, *Vol. 13*, *Page 1436* **2021**, *13* (10), 1436. <https://doi.org/10.3390/W13101436>.
- (8) *Pejão Mines, Pedorido, Castelo de Paiva, Aveiro, Portugal.* <https://www.mindat.org/loc-187014.html> (accessed 2022-09-24).
- (9) Ribeiro, J.; da Silva, E. F.; Flores, D. Burning of Coal Waste Piles from Douro Coalfield (Portugal): Petrological, Geochemical and Mineralogical Characterization. *Int. J. Coal Geol.* **2010**, *81* (4), 359–372. <https://doi.org/10.1016/j.coal.2009.10.005>.

- (10) *Regoufe Mines, Covelo de Paivó, Arouca, Aveiro, Portugal.*
<https://www.mindat.org/loc-187340.html> (accessed 2022-09-24).
- (11) *Regoufe Mines | Arouca Geopark.*
<http://aroucageopark.pt/en/know/geodiversity/geosites/regoufe-mines/> (accessed 2022-09-24).
- (12) Reis, A. T.; Rodrigues, S. M.; Davidson, C. M.; Pereira, E.; Duarte, A. C. Extractability and Mobility of Mercury from Agricultural Soils Surrounding Industrial and Mining Contaminated Areas. *Chemosphere* **2010**, *81* (11), 1369–1377. <https://doi.org/10.1016/j.chemosphere.2010.09.030>.
- (13) Frentiu, T.; Pintican, B. P.; Butaciu, S.; Mihaltan, A. I.; Ponta, M.; Frentiu, M. Determination, Speciation and Distribution of Mercury in Soil in the Surroundings of a Former Chlor-Alkali Plant: Assessment of Sequential Extraction Procedure and Analytical Technique. *Chem. Cent. J.* **2013**, *7* (1), 1–14. <https://doi.org/10.1186/1752-153X-7-178>.
- (14) Lee, P. K.; Kang, M. J.; Jo, H. Y.; Choi, S. H. Sequential Extraction and Leaching Characteristics of Heavy Metals in Abandoned Tungsten Mine Tailings Sediments. *Environ. Earth Sci.* **2012**, *66* (7), 1909–1923. <https://doi.org/10.1007/s12665-011-1415-z>.
- (15) Bacon, J. R.; Davidson, C. M. Is There a Future for Sequential Chemical Extraction? *Analyst* **2008**, *133* (1), 25–46. <https://doi.org/10.1039/b711896a>.
- (16) Dong, H.; Feng, L.; Qin, Y.; Luo, M. Comparison of Different Sequential Extraction Procedures for Mercury Fractionation in Polluted Soils. *Environ. Sci. Pollut. Res.* **2019**, *26* (10), 9955–9965. <https://doi.org/10.1007/s11356-019-04433-6>.
- (17) Pueyo, M.; Mateu, J.; Rigol, A.; Vidal, M.; López-Sánchez, J. F.; Rauret, G. Use of the Modified BCR Three-Step Sequential Extraction Procedure for the Study of Trace Element Dynamics in Contaminated Soils. *Environ. Pollut.* **2008**, *152* (2), 330–341. <https://doi.org/10.1016/j.envpol.2007.06.020>.
- (18) Rauret, G.; López-Sánchez, J. F.; Sahuquillo, A.; Rubio, R.; Davidson, C.; Ure, A.; Quevauviller, P. Improvement of the BCR Three Step Sequential Extraction Procedure Prior to the Certification of New Sediment and Soil Reference Materials. *J. Environ. Monit.* **1999**, *1* (1), 57–61. <https://doi.org/10.1039/a807854h>.
- (19) Du, X.; Gao, L.; Xun, Y.; Feng, L. Comparison of Different Sequential Extraction Procedures to Identify and Estimate Bioavailability of Arsenic Fractions in Soil. *J.*

- Soils Sediments* **2020**, 20 (10), 3656–3668. <https://doi.org/10.1007/s11368-020-02694-0>.
- (20) Wan, X.; Dong, H.; Feng, L.; Lin, Z.; Luo, Q. Comparison of Three Sequential Extraction Procedures for Arsenic Fractionation in Highly Polluted Sites. *Chemosphere* **2017**, 178, 402–410. <https://doi.org/10.1016/j.chemosphere.2017.03.078>.
- (21) Shiowatana, J.; McLaren, R. G.; Chanmekha, N.; Samphao, A. Fractionation of Arsenic in Soil by a Continuous-Flow Sequential Extraction Method. *J. Environ. Qual.* **2001**, 30 (6), 1940–1949. <https://doi.org/10.2134/jeq2001.1940>.
- (22) EPA 3200 (2014) Mercury Species Fractionation by Microwave Assisted Extraction, Selective Solvent Extraction and/or Solid Phase Extraction, U. S. Environmental Protection Agency, p.34. *Implement. Sci.* **2014**, 39 (1), 1–24.
- (23) Han, Y.; Kingston, H. M.; Boylan, H. M.; Rahman, G. M. M.; Shah, S.; Richter, R. C.; Link, D. D.; Bhandari, S. Speciation of Mercury in Soil and Sediment by Selective Solvent and Acid Extraction. *Anal. Bioanal. Chem.* **2003**, 375 (3), 428–436. <https://doi.org/10.1007/S00216-002-1701-4/TABLES/10>.
- (24) Fernández-Martínez, R.; Loredó, J.; Ordóñez, A.; Rucandio, M. I. Distribution and Mobility of Mercury in Soils from an Old Mining Area in Mieres, Asturias (Spain). *Sci. Total Environ.* **2005**, 346 (1–3), 200–212. <https://doi.org/10.1016/J.SCITOTENV.2004.12.010>.
- (25) Melaku, S.; Dams, R.; Moens, L. Determination of Trace Elements in Agricultural Soil Samples by Inductively Coupled Plasma-Mass Spectrometry: Microwave Acid Digestion versus Aqua Regia Extraction. *Anal. Chim. Acta* **2005**, 543 (1–2), 117–123. <https://doi.org/10.1016/j.aca.2005.04.055>.
- (26) CDC | Facts About Hydrogen Fluoride (Hydrofluoric Acid). <https://emergency.cdc.gov/agent/hydrofluoricacid/basics/facts.asp> (accessed 2022-08-10).
- (27) Hydrofluoric Acid Chemical Safety Information Chemical Information Overview.
- (28) Özcan, M.; Allahbeickaraghi, A.; DüNDAR, M. Possible Hazardous Effects of Hydrofluoric Acid and Recommendations for Treatment Approach: A Review. <https://doi.org/10.1007/s00784-011-0636-6>.
- (29) Santoro, A.; Held, A.; Linsinger, T. P. J.; Perez, A.; Ricci, M. Comparison of Total

- and Aqua Regia Extractability of Heavy Metals in Sewage Sludge: The Case Study of a Certified Reference Material. *TrAC - Trends Anal. Chem.* **2017**, *89*, 34–40. <https://doi.org/10.1016/J.TRAC.2017.01.010>.
- (30) Suvarapu, L. N.; Seo, Y. K.; Baek, S. O. Speciation and Determination of Mercury by Various Analytical Techniques. *Rev. Anal. Chem.* **2013**, *32* (3), 225–245. <https://doi.org/10.1515/revac-2013-0003>.
- (31) Krata, A.; Bulska, E. Critical Evaluation of Analytical Performance of Atomic Absorption Spectrometry and Inductively Coupled Plasma Mass Spectrometry for Mercury Determination. *Spectrochim. Acta - Part B At. Spectrosc.* **2005**, *60* (3), 345–350. <https://doi.org/10.1016/j.sab.2004.11.011>.
- (32) Skoog, Douglas; West, Donal M.; Holler, F. James; Crouch, S. R. *Fundamental of Analytical Chemistry*, 9th ed.; 2013.
- (33) Manuals, O. ICE 3000 Series AA. *Mercury* **2008**, *44* (1), 3000.
- (34) Pohl, P. Determination of Metal Content in Honey by Atomic Absorption and Emission Spectrometries. *TrAC Trends Anal. Chem.* **2009**, *28* (1), 117–128. <https://doi.org/10.1016/J.TRAC.2008.09.015>.
- (35) Willis, J. B. The Determination of Metals in Blood Serum by Atomic Absorption Spectroscopy—I: Calcium. *Spectrochim. Acta* **1960**, *16* (3), 259-E5. [https://doi.org/10.1016/0371-1951\(60\)80089-6](https://doi.org/10.1016/0371-1951(60)80089-6).
- (36) Murphy, V. A. Method for Determination of Sodium, Potassium, Calcium, Magnesium, Chloride, and Phosphate in the Rat Choroid Plexus by Flame Atomic Absorption and Visible Spectroscopy. *Anal. Biochem.* **1987**, *161* (1), 144–151. [https://doi.org/10.1016/0003-2697\(87\)90664-6](https://doi.org/10.1016/0003-2697(87)90664-6).
- (37) Thermo Fisher Corporation. Atomic Absorption Spectrometry Methods Manual. **2008**, *44* (5), 1–210.
- (38) Li, Z.; Yang, X.; Guo, Y.; Li, H.; Feng, Y. Simultaneous Determination of Arsenic, Antimony, Bismuth and Mercury in Geological Materials by Vapor Generation-Four-Channel Non-Dispersive Atomic Fluorescence Spectrometry. *Talanta* **2008**, *74* (4), 915–921. <https://doi.org/10.1016/j.talanta.2007.07.028>.
- (39) Ridwan, Y. S.; Ariyani, M.; Maulana, F. A.; Damara, A. F.; Pertiwi, T. Y. R. Mercury Analysis in Sediment Using Borohydric Cold Vapor Atomic Absorption Spectrometry: Performance Characteristics and Uncertainty Estimation. *IOP*

- Conf. Ser. Earth Environ. Sci.* **2022**, 1017 (1). <https://doi.org/10.1088/1755-1315/1017/1/012008>.
- (40) Campos-M, M.; Campos-C, R. Applications of Quartering Method in Soils and Foods. *Int. J. Eng. Res. Appl.* **2017**, 7 (1), 35–39. <https://doi.org/10.9790/9622-0701023539>.
- (41) ISO 12914 (2012) Soil Quality – Microwave Assisted of the Aqua Regia Soluble Fraction for the Determination of Elements, Geneva, Switzerland, p.12.
- (42) U.S. EPA. 2007. “Method 3051A (SW-846): Microwave Assisted Acid Digestion of Sediments, Sludges, and Oils,” Revision 1. Washington, DC. **2007**, No. February, 1–30.
- (43) Santoro, A.; Held, A.; Linsinger, T. P. J.; Perez, A.; Ricci, M. Trends in Analytical Chemistry Comparison of Total and Aqua Regia Extractability of Heavy Metals in Sewage Sludge : The Case Study of a Certi Fi Ed Reference Material. *Trends Anal. Chem.* **2017**, 89, 34–40. <https://doi.org/10.1016/j.trac.2017.01.010>.
- (44) ISO - ISO 8466-1:2021 - Water quality — Calibration and evaluation of analytical methods — Part 1: Linear calibration function. <https://www.iso.org/standard/77139.html> (accessed 2022-08-10).
- (45) Araujo, P. Key Aspects of Analytical Method Validation and Linearity Evaluation. *J. Chromatogr. B Anal. Technol. Biomed. Life Sci.* **2009**, 877 (23), 2224–2234. <https://doi.org/10.1016/j.jchromb.2008.09.030>.
- (46) Riley, Christopher M.; Rosanske, T. W. *Development and Validation of Analytical Methods.*; 1996.
- (47) Chen, Y. W.; Tong, J.; D’Ulivo, A.; Belzile, N. Determination of Mercury by Continuous Flow Cold Vapor Atomic Fluorescence Spectrometry Using Micromolar Concentration of Sodium Tetrahydroborate as Reductant Solution. *Analyst* **2002**, 127 (11), 1541–1546. <https://doi.org/10.1039/b207896a>.
- (48) Welna, M.; Pohl, P. Potential of the Hydride Generation Technique Coupled to Inductively Coupled Plasma Optical Emission Spectrometry for Non-Chromatographic As Speciation. *J. Anal. At. Spectrom.* **2017**, 32 (9), 1766–1779. <https://doi.org/10.1039/c7ja00107j>.
- (49) Helena, L. U. Z.; Rodríguez, S. Determinación Comparativa De Mercurio Total En Cabello Por Espectroscopías De Absorción Atómica Con Generador De Hidruros

Y Diferencial De Efecto Zeeman Con Pirolizador. **2009**.

- (50) *Foregs Geochemical Atlas*. <http://weppi.gtk.fi/publ/foregsatlas/> (accessed 2022-08-23).
- (51) APA. Valores De Referência Para O Solo. *Solos Contam. - Guia Técnico* **2019**, 2019, 1–73.
- (52) Birch, G. *Use of Sedimentary-Metal Indicators in Assessment of Estuarine System Health*; Elsevier Ltd., 2013; Vol. 14. <https://doi.org/10.1016/B978-0-12-374739-6.00392-4>.
- (53) Ilman, M.; Abdullah, C.; Shah, A.; Sah, R. M.; Haris, H. Geoaccumulation Index and Enrichment Factor of Arsenic in Surface Sediment of Bukit Merah Reservoir, Malaysia Authors. *TLSR* 31 (3), 2020. <https://doi.org/10.21315/tlsr2020.31.3.8>.
- (54) Mashyanov, N. R.; Pogarev, S. E.; Panova, E. G.; Panichev, N.; Ryzhov, V. Determination of Mercury Thermospecies in Coal. *Fuel* **2017**, 203, 973–980. <https://doi.org/10.1016/j.fuel.2017.03.085>.
- (55) Liu, X.; Bai, Z.; Shi, H.; Zhou, W.; Liu, X. Heavy Metal Pollution of Soils from Coal Mines in China. *Nat. Hazards* **2019**, 99 (2), 1163–1177. <https://doi.org/10.1007/s11069-019-03771-5>.
- (56) Li, X.; Huang, L. Toward a New Paradigm for Tailings Phytostabilization - Nature of the Substrates, Amendment Options, and Anthropogenic Pedogenesis. *Crit. Rev. Environ. Sci. Technol.* **2015**, 45 (8), 813–839. https://doi.org/10.1080/10643389.2014.921977/SUPPL_FILE/BEST_A_921977_SM9747.ZIP.

Annex I – Preliminary results for As and Sb

The pseudo-total concentration of As and Sb were determined for the samples collected in the waste pile affected by fire in the Fojo region. The obtained values are summarized at the **Table 15A1** and also represented in **Figure Al.1** and **Figure Al.2**.

Table 151 - Hg aqua regia soluble content for Regoufe mine samples.

Amostra	As (mg.kg ⁻¹) (± 4 mg.kg ⁻¹) ^(a)	Sb (mg.kg ⁻¹) (± 0.8 mg.kg ⁻¹) ^(a)
EA1	38.8	6.5
EA2	31.0	5.8
EA3	41.2	5.2
EA4	38.3	6.5
EA5	42.7	5.3
EA6	46.4	4.9
EA7	38.4	6.0
EA8	40.6	5.2
EA9	46.8	4.8
EA10	68.6	8.3
Média	43	6
sb	10	1
Min	31.0	4.8
Max	68.6	8.3

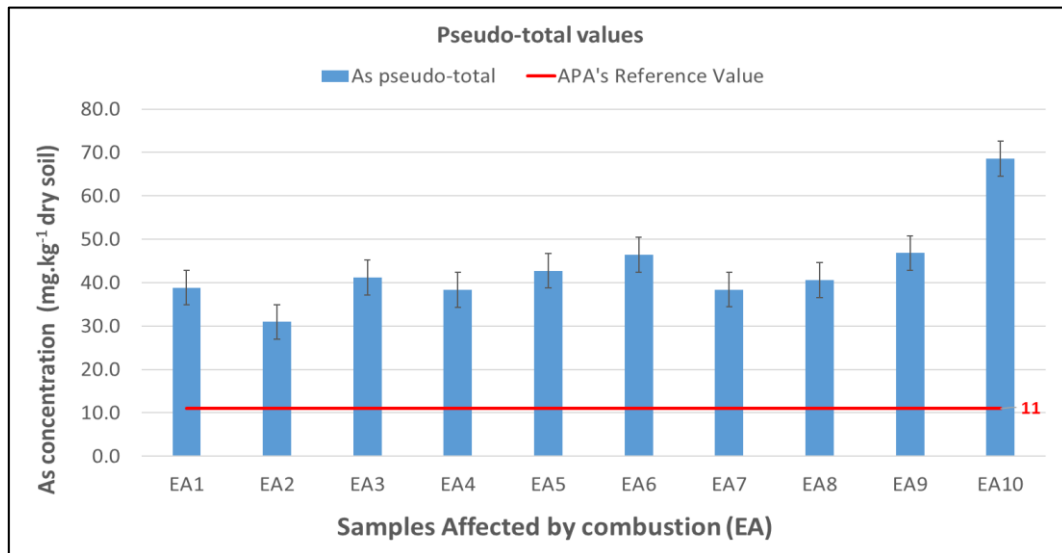


Figure Al.1 - Graphical representation of the obtained *aqua regia* soluble content of As in samples affected by combustion of the Pejão coal mine. APA reference value is represented by the red line.

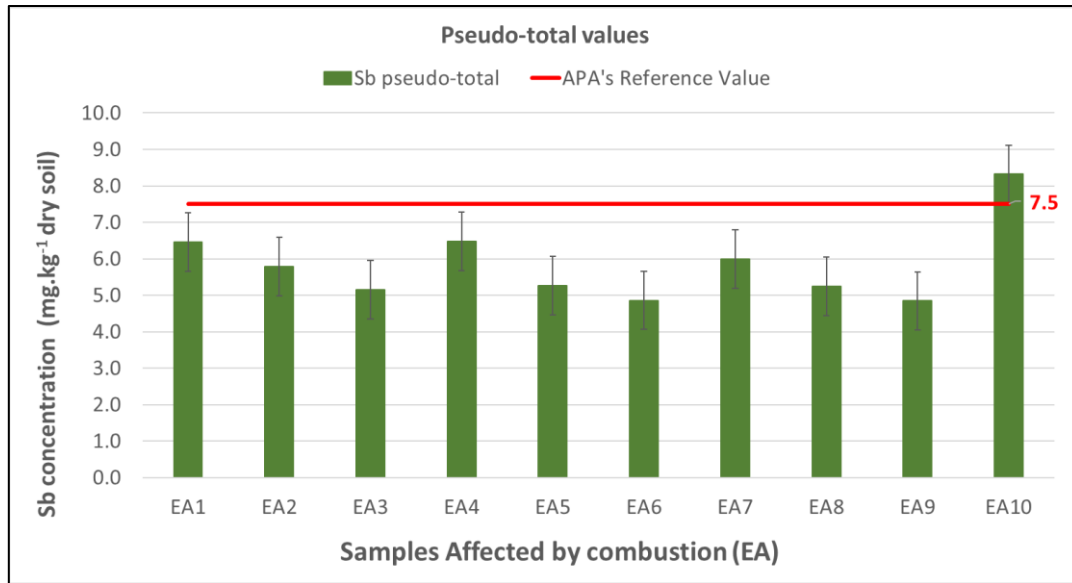


Figure Al.2 - Graphical representation of the obtained *aqua regia* soluble content of Sb in samples affected by combustion of the Pejão coal mine. APA reference value is represented by the red line.

The obtained values for As and Sb in the analyzed soil samples, ranging from 31.0 to 68.6 mg.Kg⁻¹ and 4.8 to 8.3 mg.kg⁻¹, respectively, are above the European background values reported in project FOREGS (11.6 mg.kg⁻¹ for As and 1.04 mg.kg⁻¹ for Sb)^[50] showing a significant enrichment of these PTEs, being a potential source of contamination in the mine region.

Relatively to the APA's reference values for agricultural soils all samples showed concentration values of As significantly above the suggested value (11 mg.kg⁻¹) and for Sb samples EA1, EA4 and EA10 revealed values either very close or above the reference value (7.5 mg.kg⁻¹). Therefore, speciation of both PTEs is recommended.

Annex II – As and Sb SEP method

The method for arsenic fractionating described below consists of a five-step procedure. Bioavailable As in soils are roughly classified into mobile and stable fraction. As species classified into the mobile fraction are those that, subjected to specific environmental conditions, can be converted to a free state (or that already exists freely in soils) and the remaining species are classified into the stable fraction. According to this classification, the acid-extracted fraction is generally considered to be most bioavailable fraction (steps 1,2 and 4).

Sb species generally show similar reactivity to As species and, as such, this SEP was considered to be adequate for the fractioning of Sb in soils as well.

All.1. Water soluble-extractable species – Step 1

To 1.0 ± 0.5 g of homogenized sub-sample was added 30.0 mL of pure water in a 50 mL centrifuge tube. The suspension was shaken for 16 h using a ScanSci SK-300-pro linear shaker at 200 rpm and posteriorly centrifuged at 3200 rpm for 15 min. The supernatant was filtered through a 0.45 μm NY membrane syringe filter and diluted with pure water to a final volume of 50 mL before analysis by Hydride Generation Atomic Absorption Spectrometry (HG-AAS).

All.2. Sodium bicarbonate-extractable species – Step 2

The soil residue from the previous step was washed with 30 mL of DDI water, centrifuged and the supernatant discarded. Then, the residue was resuspended in 30 mL of NaHCO_3 (0.5 mol.L^{-1}) and shaken for 16 h. After that, the suspension was centrifuged and filtered as in step 1 prior to analysis.

All.3. Sodium hydroxide-extractable species – Step 3

The soil residue from the previous step was washed with 30 mL of pure water, centrifuged and the supernatant discarded. Then, the residue was resuspended in 30.0 mL of NaOH (0.1 mol.L^{-1}) and shaken for 16 h. After that, the suspension was centrifuged and filtered as in step 1 prior to analysis.

All.4. Hydrochloric acid-extractable species – Step 4

The soil residue from the previous step was washed with 30 mL of pure water, centrifuged and the supernatant discarded. Then the residue was resuspended in 30.0 mL of HCl (1 mol.L⁻¹) and shaken for 16 h. After that, the suspension was centrifuged and filtered as in step 1 prior to analysis.